Bulletin of the Seismological Society of America, Vol. 84, No. 5, pp. 1410–1442, October 1994

Theoretical Rayleigh and Love Waves from an Explosion in Prestressed Source Regions

by D. G. Harkrider, J. L. Stevens, and C. B. Archambeau

Abstract Expressions and synthetics for Rayleigh and Love waves generated by theoretical tectonic release models are presented. The multipole formulas are given in terms of the strengths and time functions of the source potentials. This form of the Rayleigh and Love wave expressions is convenient for separating the contribution to the Rayleigh wave due to the compressional and shear-wave source radiation and the contribution of the upgoing and downgoing source radiation for both Rayleigh and Love waves. Because of the ease of using different compression and shear-wave source time functions, these formulas are especially suited for sources for which second- and higher-order moment tensors are needed to describe the source, such as the initial value cavity release problem.

A frequently used model of tectonic release is a double couple superimposed on an explosion. Eventually, we will compare synthetics of this and more realistic models in order to determine for what dimensions of the tectonic release model this assumption is valid and whether the Rayleigh wave is most sensitive to the compressional or shear-wave source history. The pure shear cavity release model is a double couple with separate *P*- and *S*-wave source histories. The time scales are proportional to the source region's dimension and differ by their respective body-wave velocities. Thus, a convenient way to model the effect of differing shot point velocities and source dimensions is to run a suite of double-couple source history calculations for the *P*- and *SV*-wave sources separately and then sum the different combinations.

One of the more interesting results from this analysis is that the well-known effect of vanishing Rayleigh-wave amplitude as a vertical or horizontal dip-slip double-couple model approaches the free surface is due to the destructive interference between the *P*- and *SV*-wave generated Rayleigh waves. The individual Rayleigh-wave amplitudes, unlike the *SH*-generated Love waves, are comparable in size to those from other double-couple orientations. This has important implications to the modeling of Rayleigh waves from shallow dip-slip fault models. Also, the *P*-wave radiation from double-couple sources is a more efficient generator of Rayleigh waves than the associated *SV* wave or the *P* wave from explosions. The latter is probably due to the vertical radiation pattern or amplitude variation over the wave front. This effect should be similar to that of the interaction of wave-front curvature with the free surface.

Introduction

A frequently used model of tectonic release from underground nuclear explosions is a double couple superimposed on an explosion. For a point double couple, the time functions or histories for the source compressional (*P*) and shear (*S*) waves are identical. For more realistic models of tectonic release, such as the formation of a cavity in a pure shear field, the source radiation pattern is identical to a double couple but the *P*- and *S*-wave source histories differ. We restrict tectonic release to explosion-induced volume relaxation sources in a prestressed medium and do not consider earthquake triggering by an explosion. For a spherical cavity, the *P*- and *S*-wave time scales are roughly proportional to the cavity dimensions and differ by their respective body-wave velocities. We will show that Rayleigh waves excited by the source *P* waves are almost completely out

of phase with the S-wave generated Rayleigh waves, and thus this difference in source histories may in some cases be important.

We present expressions and synthetics for Rayleigh and Love waves generated by various tectonic release models. The multipole formulas are given in terms of the strengths and time functions of the source potentials. This form of the Rayleigh- and Love-wave expressions is convenient for separating the contribution to the Rayleigh wave from the P- and S-wave source radiation and the contribution of the upgoing and downgoing source radiation for both Rayleigh and Love waves. Because of the ease of using different compression and shear-wave source time functions, these formulas are especially suited for sources for which second- and higher-order moment tensors (Backus and Mulcahy, 1976; Stump and Johnson, 1977; Doornbos, 1982; Stump and Johnson, 1982) are needed to describe the source, such as the initial value problem of the instantaneous formation of a cavity in a prestressed medium (Ben-Menahem and Singh, 1981, pp. 221–229).

In 1964, Haskell and Harkrider presented formulations for sources and receivers in multilayered isotropic half-spaces. The formulations were for general point sources, which were simplified for particular sources. Haskell gave the results for point forces, dipoles, couples, double couples and explosions. Harkrider gave expressions for the surface waves from explosions and Green's functions, i.e., point forces. Both formulations used propagator matrices for homogeneous isotropic layers. Ben-Menahem and Harkrider (1964) extended the far-field results of Harkrider (1964) to couples and double couples of arbitrary orientation.

Other than the sources investigated, the basic difference between the results was that Haskell propagated from the source up to the free surface, while Harkrider obtained the source and receiver depth effects in terms of layer propagators from the surface down to the source as well as the receiver. To obtain the latter result, Harkrider used an inverse for the homogeneous layer propagators, which formed a matrix sub-group; i.e., the inverse of the product of two layer propagator matrices was related in the same way to the elements of the product as the inverse of each layer matrix was to the elements of the homogeneous layer matrix. This is not true for the homogeneous layer inverse, which is produced by replacing the layer thickness with the negative layer thickness (Haskell, 1953). The inverse used by Harkrider allowed him to replace the terms involving propagation up from the source as in Haskell with terms of downward propagation to the source. The extra effort was made in order to put the results in terms of quantities routinely calculated in homogeneous, i.e., no source, surface-wave dispersion programs and in order to demonstrate reciprocity. Each formulation has advantages. Harkrider (1970) reduced the numerical problems of his formulation by evaluating his expressions using the compound matrix relations of Dunkin (1965) and Gilbert and Backus (1966). Further numerical improvements to layer matrix methods can be found in Kind and Odom (1983).

Hudson (1969) extended the formulation of Haskell (1964) to propagators for isotropic vertically inhomogeneous velocity and density structures. Since Haskell's formulation did not use inverse propagators, this was relatively straightforward. Douglas *et al.* (1971) used reciprocity relations with Hudson's formulation to obtain the vertically inhomogeneous results for explosions equivalent to Harkrider's multilayer result. It was not until the middle 1970s that Woodhouse (1974) showed that this inverse was true for the more general isotropic inhomogeneous half-space.

Ben-Menahem and Singh (1968a,b) presented a formulation using multipolar expansions of the displacement Hansen vectors. We use a similar multipolar expansion of the scalar potentials for P, SV, and SH waves. Since numerical finite-difference simulations of complex source or source region radiation routinely use the divergence and curl of the displacement field to separate P- and S-wave radiation and since these are easily related to P- and S-wave potentials, this type of expansion was a natural one for this class of problem. This was the original motivation for using potential expansions (Bache and Harkrider, 1976). In addition, it allowed us to use the theoretical results of Harkrider (1964) for Rayleigh and Love waves in multilayered media by means of a trivial generalization. For theoretical problems, the choice between multipolar expansion of Hansen vectors and potentials is a matter of convenience. In fact, we use the Hansen vector representation of the displacement field for a cavity-initiated tectonic release as our fundamental source and then convert it into potentials.

This formulation, either in preliminary drafts of this manuscript or as a part of technical reports, has been referenced and/or used by Bache and Harkrider (1976), Bache *et al.* (1978), Harkrider (1981), and Stevens (1982). The prestress fields discussed in this article are restricted to homogeneous pure shear fields. More complicated cases can be found in Stevens (1980, 1982).

In the next section we present the displacement fields and potentials for the tectonic release source and the various approximations to it that have appeared in the literature, including the point double couple. In addition, we give the displacements and potentials for the explosion model corresponding to a step pressure applied to a spherical cavity. The sources are discussed in terms of their equivalent moment tensor forms and we present illustrative comparisons of their far-field time functions. In the following sections, we present the multipole source extension to the explosion and point force formulation of Harkrider (1964) and then evaluate it to obtain surface-wave expressions for the sources mentioned above. We also obtain expressions for the canonical second-or-

der moment tensor for comparison with Mendiguren (1977). Finally, we calculate Rayleigh- and Love-wave seismograms for canonical orientations of the pure shear stress field (Harkrider, 1977) and discuss them in terms of their P- and S-wave excitation.

Tectonic Release Source Models

We start this section with a presentation of the seismic radiation from our preferred tectonic release source in a form that allows us to interpret it in its lowest order of moment tensor. Even though the result is in terms of moment tensors of order greater than two, we can keep it in a second-order or double-couple form if it is separated into two Green's functions with different moment histories. Next, we determine the multipole representation for this source. A special case of this radiation is the double-couple model of earthquakes for which the moment histories are equal. The histories for the instantaneous or supersonic cavity growth model of tectonic release are uniquely determined by the elastic properties at the source and the cavity radius. For an earthquake model, we have to specify the slip history. For comparison purposes, we give the slip history for a simple source that allows us to specify spectral corner frequencies similar to the cavity release model. For completeness and comparison, we also give two explosion source histories.

Stevens (1980) presented the theory and numerical calculations of the seismic radiation that would be produced by the sudden creation of a spherical cavity in an arbitrary prestressed medium. The stress fields considered were both homogeneous and inhomogeneous with stress concentrations. Because of the finiteness of the cavity, even placing it at a location of symmetry with respect to the stress concentrations or in a homogeneous pure shear field required a multipole source description of order two or a combination of moment tensors of order greater than two. Other than the trivial example of a monopole due to a pure compression, the simplest source radiation was that for a cavity introduced into a homogeneous pure shear-stress field. The resulting radiation could be represented by a multipole of order two for the P and S waves but required a different history for each. The histories for this simple source geometry were scaled by the radius of the cavity divided by the P and S velocities. Stevens also pointed out that the only analytic description for the more complicated models is a multipole formulation. Details on the behavior of these models and the literature associated with their development can be found in Stevens (e.g., Burridge, 1975; Burridge and Alterman, 1972; Hirasawa and Sato, 1963; Koyama et al., 1973; Sezawa and Kanai, 1941, 1942).

The simplest tectonic release source, which has an earthquakelike radiation pattern, the complications of finiteness, and a deterministic source history, is the instantaneous creation of a spherical cavity of radius R_0 in the presence of pure shear, $\tau_{12}^{(0)}$, at infinity. The form of the solution used here and the notation are from Ben-Menahem and Singh (1981, p. 228).

$$\bar{\mathbf{u}}(\mathbf{x}, \omega) = \gamma_{22}^S \mathbf{L}_{22}^S(k_\alpha R) + \beta_{22}^S \mathbf{N}_{22}^S(k_\beta R), \tag{1}$$

where the Hansen vectors are

$$\mathbf{L}_{22}^S(k_\alpha R) = \frac{dh_2^{(2)}(k_\alpha R)}{d(k_\alpha R)} \mathbf{P}_{22}^S + \frac{h_2^{(2)}(k_\alpha R)}{(k_\alpha R)} \sqrt{6}\, \mathbf{B}_{22}^S$$

$$\mathbf{N}_{22}^S(k_\beta R) = 6 \frac{h_2^{(2)}(k_\beta R)}{(k_\beta R)} \mathbf{P}_{22}^S + \left[\frac{dh_2^{(2)}(k_\beta R)}{d(k_\beta R)} + \frac{h_2^{(2)}(k_\beta R)}{(k_\beta R)} \right] \sqrt{6}\, \mathbf{B}_{22}^S \tag{2}$$

and the vector spherical harmonics are

$$\mathbf{P}_{22}^S = P_2^2(\cos\theta) \sin 2\phi\, \mathbf{e}_R$$

$$\sqrt{6}\, \mathbf{B}_{22}^S = 2\, P_2^1(\cos\theta) \sin 2\phi\, \mathbf{e}_\theta + 6\, P_1^1(\cos\theta) \cos 2\phi\, \mathbf{e}_\phi. \tag{3}$$

The coefficients are given by

$$\beta_{22}^S = -\frac{\tau_{12}^{(0)}}{6\mu k_\beta} g(\omega) \frac{[2F_{2,1}(k_\alpha R_0) - F_{2,3}(k_\alpha R_0)]}{\Delta_2}$$

$$\gamma_{22}^S = -\frac{\tau_{12}^{(0)}}{6\mu k_\alpha} g(\omega) \frac{[6F_{1,2}(k_\beta R)_0 - F_{2,2}(k_\beta R_0)]}{\Delta_2}, \tag{4}$$

where

$$F_{l,1}(\xi) = \frac{(l-1)}{\xi^2} h_l^2(\xi) - \frac{1}{\xi} h_{l+1}^{(2)}(\xi)$$

$$F_{l,2}(\xi) = \left[\frac{2}{\xi^2}(l^2 - 1) - 1 \right] h_l^{(2)}(\xi) + \frac{2}{\xi} h_{l+1}^{(2)}(\xi)$$

$$F_{l,3}(\xi) = \left[\frac{1}{\xi^2} l(l-1) - \frac{1}{2}\left(\frac{\alpha}{\beta}\right)^2 \right] h_l^{(2)}(\xi) + \frac{2}{\xi} h_{l+1}^{(2)}(\xi)$$

$$\Delta_l = 2l(l+1) F_{l,1}(k_\beta R_0) F_{l,1}(k_\alpha R_0) - F_{l,2}(k_\beta R_0) F_{l,3}(k_\alpha R_0) \tag{5}$$

and

$$g(\omega) = \frac{1}{i\omega}.$$

In cylindrical coordinates, the Hansen vectors are given by

$$\mathbf{L}^S_{22}(k_\alpha R) = \frac{1}{k_\alpha}\nabla[h_2^{(2)}(k_\alpha R)P_2^2(\cos\theta)\sin 2\phi]$$

and

$$\mathbf{N}^S_{22}(k_\beta R) = -\frac{2}{k_\beta}\nabla[h_2^{(2)}(k_\beta R)P_2^2(\cos\theta)\sin 2\phi] + 6\,h_1^{(2)}(k_\beta R)P_1^1(\cos\theta)(\sin\phi\,\mathbf{e}_1 + \cos\phi\,\mathbf{e}_2). \tag{6}$$

Using the following relations,

$$\frac{\partial A_v}{\partial x_1} = ik_v^2\,h_1^{(2)}(k_vR)P_1^1(\cos\theta)\cos\phi$$

$$\frac{\partial A_v}{\partial x_2} = ik_v^2\,h_1^{(2)}(k_vR)P_1^1(\cos\theta)\sin\phi$$

$$\frac{\partial^2 A_v}{\partial x_1\partial x_2} = -ik_v^3\,h_2^{(2)}(k_vR)P_2^2(\cos\theta)\sin 2\phi, \tag{7}$$

where

$$A_v = -ik_vh_0^{(2)}(k_vR) = \frac{\exp(-ik_vR)}{R},$$

we have

$$\mathbf{L}^S_{22}(k_\alpha R) = i\frac{6}{k_\alpha^4}\left\{\nabla\frac{\partial^2 A_\alpha}{\partial x_1\partial x_2}\right\}$$

$$\mathbf{N}^S_{22}(k_\beta R) = -i\frac{6}{k_\beta^4}\left\{2\,\nabla\frac{\partial^2 A_\beta}{\partial x_1\partial x_2} + k_\beta^2\left(\frac{\partial A_\beta}{\partial x_2}\mathbf{e}_1 + \frac{\partial A_\beta}{\partial x_1}\mathbf{e}_2\right)\right\} \tag{8}$$

and we can write the Cartesian components of displacement as

$$\bar{u}_i(\mathbf{x},\omega) = i\left[\frac{K_\alpha}{k_\alpha^3}2\frac{\partial^3 A_\alpha}{\partial x_i\partial x_1\partial x_2} - \frac{K_\beta}{k_\beta^3}\left\{2\frac{\partial^3 A_\beta}{\partial x_i\partial x_1\partial x_2} + k_\beta^2\left(\frac{\partial A_\beta}{\partial x_2}\delta_{i1} + \frac{\partial A_\beta}{\partial x_1}\delta_{i2}\right)\right\}\right] \tag{9}$$

where

$$K_\alpha = \frac{3}{k_\alpha}\gamma^S_{22}$$

and

$$K_\beta = \frac{6}{k_\beta}\beta^S_{22}. \tag{10}$$

This solution in spectral moment tensor form is

$$\bar{u}_i(\mathbf{x},\omega) = -\left[\bar{M}_{12}(\bar{G}_{i1,2} + \bar{G}_{i2,1}) + \frac{1}{6}\bar{M}_{1112}\bar{G}_{ip,p12}\right], \tag{11}$$

where the moment tensor components are

$$\bar{M}_{12}(\omega) = \bar{M}_{21}(\omega) = i\,4\pi\rho\omega^2\frac{K_\beta}{k_\beta^3} \tag{12}$$

$$\bar{M}_{1112}(\omega) = \bar{M}_{2212}(\omega) = \bar{M}_{3312}(\omega) = -i\frac{48\pi\rho\omega^2}{k_\alpha^2}\left(\frac{K_\alpha}{k_\alpha^3} - \frac{K_\beta}{k_\beta^3}\right) \tag{13}$$

since

$$\bar{G}_{ij,k}(\omega) = \frac{1}{4\pi\rho\omega^2}\left\{\frac{\partial^3(A_\beta - A_\alpha)}{\partial x_i\partial x_j\partial x_k} + \delta_{ij}k_\beta^2\frac{\partial A_\beta}{\partial x_k}\right\} \tag{14}$$

and

$$\bar{G}_{ip,p12}(\omega) = \frac{\partial^2}{\partial x_1\partial x_2}(\bar{G}_{i1,1} + \bar{G}_{i2,2} + \bar{G}_{i3,3}) = \frac{1}{4\pi\rho\omega^2}k_\alpha^2\frac{\partial^3 A_\alpha}{\partial x_i\partial x_1\partial x_2} \tag{15}$$

and

$$\bar{G}_{i1,2} + \bar{G}_{i2,1} = \frac{1}{4\pi\rho\omega^2}\left\{2\frac{\partial^3(A_\beta - A_\alpha)}{\partial x_i\partial x_1\partial x_2} + k_\beta^2\left(\delta_{i1}\frac{\partial A_\beta}{\partial x_2} + \delta_{i2}\frac{\partial A_\beta}{\partial x_1}\right)\right\}. \tag{16}$$

Thus, the lowest order of moment tensor, which this source can be expressed as, is a second-order plus a fourth-order moment tensor (David Cole, 1982, personal comm.).

From Ben-Menahem and Singh (1981), as $\omega \to 0$

$$\frac{K_\beta}{k_\beta^3} \to -\frac{1}{\omega}\frac{\pi\tau_{12}^{(0)}}{4\pi\rho\omega^2}R_0^3\frac{(1-\sigma)}{(7-5\sigma)}\left\{20 + \frac{(1-3\sigma)}{(1-2\sigma)}\frac{\omega^2}{\alpha^2}R_0^2\right\}, \tag{17}$$

where σ is Poisson's ratio. Substituting this limit, we have

$$\bar{M}_{12}(\omega) \to \frac{1}{i\omega} 20\pi\tau_{12}^{(0)} R_0^3 \frac{(1-\sigma)}{(7-5\sigma)}. \tag{18}$$

From the definition of scalar moment,

$$M_0 = \lim_{\omega \to 0} \{i\omega \bar{M}_{12}(\omega)\} = 20\pi\tau_{12}^{(0)} R_0^3 \frac{(1-\sigma)}{(7-5\sigma)}, \tag{19}$$

which is the same result obtained from the approximate solutions to this problem given by Randall (1966) and Archambeau (1972) (Aki and Tsai, 1972; Randall, 1973a, b; Harkrider, 1976; Minster and Suteau, 1977; Minster, 1979).

Also,

$$\frac{K_\alpha}{k_\alpha^3} \to -\frac{1}{\omega} \frac{\pi\tau_{12}^{(0)}}{4\pi\rho\omega^2} R_0^3 \frac{(1-\sigma)}{(7-5\sigma)} \left\{ 20 + \frac{3}{2} \frac{\omega^2}{\beta^2} R_0^2 \right\} \tag{20}$$

and

$$\bar{M}_{1112}(\omega) = -i\, 48\pi\rho\alpha^2 \left\{ \frac{K_\alpha}{k_\alpha^3} - \frac{K_\beta}{k_\beta^3} \right\}$$

$$\to \frac{1}{i\omega} 24\pi\tau_{12}^{(0)} R_0^5 \frac{(1-\sigma)}{(1-2\sigma)(7-5\sigma)} \tag{21}$$

as $\omega \to 0$.

This higher-order moment tensor complexity is simply due to the P-wave history being different than the S-wave. This difference in histories is not unusual and is typically due to source finiteness, as here. Because of the source volume symmetry, it is not a function of take-off angle and azimuth such as is in the case of fault plane directivity. We can keep the double couple, and more generally the second-order moment tensor formulation, if we separate the Green's function into its P- and S-wave contributions and define separate P- and S-wave moment tensor components. For this case, $\bar{M}_{12}^{(P)}(\omega)$ and $\bar{M}_{12}^{(S)}(\omega)$ are

$$\bar{M}_{12}^{(P)}(\omega) = i\, 4\pi\rho\omega^2 \frac{K_\alpha}{k_\alpha^3}$$

and

$$\bar{M}_{12}^{(S)}(\omega) = i\, 4\pi\rho\omega^2 \frac{K_\beta}{k_\beta^3} \tag{22}$$

as in equation (12), with corner frequencies

$$f_c^{(P)} = \frac{\alpha}{2\pi R_0} \left[\frac{(7-5\sigma)}{5(1-\sigma)} \right]^{1/2}$$

and

$$f_c^{(S)} = \frac{\beta}{2\pi R_0} \left[\frac{(7-5\sigma)}{5(1-\sigma)} \right]^{1/2}$$

and their respective whole space Green's functions

$$\bar{G}_{i1,2}^{(P)} + \bar{G}_{i2,1}^{(P)} = -\frac{1}{4\pi\rho\omega^2} 2 \frac{\partial^3 A_\alpha}{\partial x_i \partial x_1 \partial x_2}$$

and

$$\bar{G}_{i1,2}^{(S)} + \bar{G}_{i2,1}^{(S)} = \frac{1}{4\pi\rho\omega^2} \left\{ 2 \frac{\partial^3 A_\beta}{\partial x_i \partial x_1 \partial x_2} + k_\beta^2 \left(\delta_{i1} \frac{\partial A_\beta}{\partial x_2} + \delta_{i2} \frac{\partial A_\beta}{\partial x_1} \right) \right\}. \tag{23}$$

Except for the time functions, this is the same result obtained for the Randall–Archambeau approximate solution to this problem. Their spectral histories in this notation, after correcting for a sign error in the stress definition in Harkrider (1976), are

$$K_\nu = \frac{3M_0}{4\pi\rho\omega^2} \frac{\omega^2}{\nu} \frac{D(k_\nu R_0)}{\omega^2 R_0^2} \tag{24}$$

where M_0 is given by equation (19) and

$$D(x) = \cos x - \frac{\sin x}{x}$$

with corner frequencies

$$f_c^{(P)} = \frac{\sqrt{3}\,\alpha}{2\pi R_0}$$

and

$$f_c^{(S)} = \frac{\sqrt{3}\,\beta}{2\pi R_0}.$$

For these tectonic release sources, the far-field rise times for P and S are given by $T_0^{(\alpha)} = R_0/\alpha$ and $T_0^{(\beta)} = R_0/\beta$, respectively.

Because of the form of this elastic whole space solution, P- and S-wave separation is trivial. For more complicated sources, a Green's function separation can be done naturally using the multipole P- and S-wave po-

tential formulation of the next sections. The potentials can then be substituted into our multipole expressions for a vertically inhomogeneous half-space in order to obtain Rayleigh and Love waves.

We could obtain the desired source description in terms of the scalar compression potential, $\mathbf{\Phi}$, and the shear rotation vector potentials, $\mathbf{\Psi}$, by the following operations:

$$\bar{\mathbf{\Phi}} = -\frac{1}{k_\alpha^2} \nabla \cdot \mathbf{u}(\mathbf{x}, \omega)$$

and

$$\bar{\mathbf{\Psi}} = \frac{1}{k_\beta^2} \nabla \times \mathbf{u}(\mathbf{x}, \omega) \tag{25}$$

on the displacement expressions, equation (1), as was done for the second-rank seismic moment tensor in Appendix D. For more complicated sources, especially those for which there is no analytic representation, this is a very convenient and practical method.

But equations (1) and (2) are already in the form of the general quadrupole of Harkrider (1976),

$$\bar{u}_R = \sin^2\theta \sin 2\phi \left\{ K_\alpha \frac{d}{dR} h_2^{(2)}(k_\alpha R) + 3K_\beta \frac{h_2^{(2)}(k_\beta R)}{R} \right\}$$

$$\bar{u}_\theta = \sin 2\theta \sin 2\phi \left\{ K_\alpha \frac{h_2^{(2)}(k_\alpha R)}{R} + \frac{1}{2} K_\beta \left[\frac{d}{dR} h_2^{(2)}(k_\beta R) + \frac{h_2^{(2)}(k_\beta R)}{R} \right] \right\}$$

$$\bar{u}_\phi = \sin\theta \cos 2\phi \left\{ 2K_\alpha \frac{h_2^{(2)}(k_\alpha R)}{R} + K_\beta \left[\frac{d}{dR} h_2^{(2)}(k_\beta R) + \frac{h_2^{(2)}(k_\beta R)}{R} \right] \right\}. \tag{26}$$

Comparing equation (26) with equations (49) and (50) of Harkrider (1976), we can write down the Cartesian displacement potentials [Harkrider, 1976, equation (47)] for this class of source as

$$\bar{\mathbf{\Phi}} = K_\alpha \sin^2\theta \sin 2\phi \, h_2^{(2)}(k_\alpha R)$$

$$\bar{\mathbf{\Psi}}_1 = K_\beta \cos\theta \sin\theta \cos\phi \, h_2^{(2)}(k_\beta R)$$

$$\bar{\mathbf{\Psi}}_2 = -K_\beta \cos\theta \sin\theta \sin\phi \, h_2^{(2)}(k_\beta R)$$

$$\bar{\mathbf{\Psi}}_3 = -K_\beta \sin^2\theta \cos 2\phi \, h_2^{(2)}(k_\beta R) \tag{27}$$

or

$$\bar{\mathbf{\Phi}} = \frac{K_\alpha}{3} P_2^2(\cos\theta) \sin 2\phi \, h_2^{(2)}(k_\alpha R)$$

$$\bar{\mathbf{\Psi}}_1 = \frac{K_\beta}{3} P_2^1(\cos\theta) \cos\phi \, h_2^{(2)}(k_\beta R)$$

$$\bar{\mathbf{\Psi}}_2 = -\frac{K_\beta}{3} P_2^1(\cos\theta) \sin\phi \, h_2^{(2)}(k_\beta R)$$

$$\bar{\mathbf{\Psi}}_3 = -\frac{K_\beta}{3} P_2^2(\cos\theta) \cos 2\phi \, h_2^{(2)}(k_\beta R) \tag{28}$$

and for the dislocation slip history, we use the Ohnaka (1973) form of the "ω-square" model (Harkrider, 1976), which is the minimum phase history of ω-square source spectra (Aki, 1967). In the far-field, its radiation is identical to Brune's (1970) earthquake source radiation. In terms of spectral moment history, it is given by

$$\bar{M}(\omega) = \frac{k_T^2 M_0}{i\omega(k_T + i\omega)^2}$$

with corner frequency

$$f_c = \frac{1}{2\pi T_0}$$

and

$$K_\nu = -\frac{M_0}{4\pi\rho\omega^2} \frac{1}{\nu} \frac{k_T^2}{(k_T + i\omega)^2} k_\nu^2. \tag{29}$$

For both P and S waves, the far-field rise time is given by $T_0 = 1/k_T$.

The source histories of explosions are usually expressed in terms of their reduced displacement potentials $\Psi(t)$, which is implicitly defined by the explosion's linear displacement radiation field as

$$u_R = -\frac{\partial}{\partial R} \frac{\Psi(t - R/\alpha)}{R}.$$

Since

$$u_R = \frac{\partial}{\partial R} \bar{\mathbf{\Phi}},$$

we have

$$\bar{\mathbf{\Phi}} = i \, \bar{\Psi}(\omega) k_\alpha h_0^{(2)}(k_\alpha R). \tag{30}$$

For consistency with the second-order moment tensor, we have

$$\bar{M}(\omega) = \bar{M}_{11} = \bar{M}_{22} = \bar{M}_{33} = 4\pi\rho\alpha^2\bar{\Psi}(\omega).$$

We will only consider two explosion source histories; the step moment,

$$\bar{M}(\omega) = \frac{M_0}{i\omega}, \tag{31}$$

and

$$\bar{M}(\omega) = \frac{M_0}{i\omega} \frac{e^{i(k_\alpha R_0 - \theta_B)}}{[(1 - k_\beta^2 R_0^2/4)^2 + k_\alpha^2 R_0^2]^{1/2}}, \tag{32}$$

where

$$\theta_B = \tan^{-1} \frac{k_\alpha R_0}{(1 - k_\beta^2 R_0^2/4)}$$

with corner frequency

$$f_c = \frac{\beta}{\pi R_0},$$

which corresponds to a step pressure applied to the walls of a cavity of radius R_0.

In Figure 1, we show the far-field radial (P) and tangential (S) displacement histories for the exact tectonic cavity release, for the Randall–Archambeau approximate cavity release, and for the ω-square double-couple model. The cavity radius is the same for the first two models and the P and S rise times for the double couple are chosen to be the same as the cavity release S rise times. This is more evident in Figure 2 where we show the corresponding P- and S-wave velocity fields. The moment is the same for all the sources. The S-wave velocity fields for the cavity release and the double couple are very similar. The basic difference is in the time duration and amplitude of their P-wave fields. In Figure 3, we compare the P- and S-wave displacement fields in detail for these three sources by overlaying them and having the same moment for each comparison. The moments for the P waves are greater than the S waves in order to display better the differences in wave form.

In Figure 4, we compare the P-wave, i.e., radial, displacement and velocity fields for the tectonic cavity release and the cavity step pressure explosion for the same moment and cavity radius. The histories are quite similar, with the basic difference being the distortion or bump

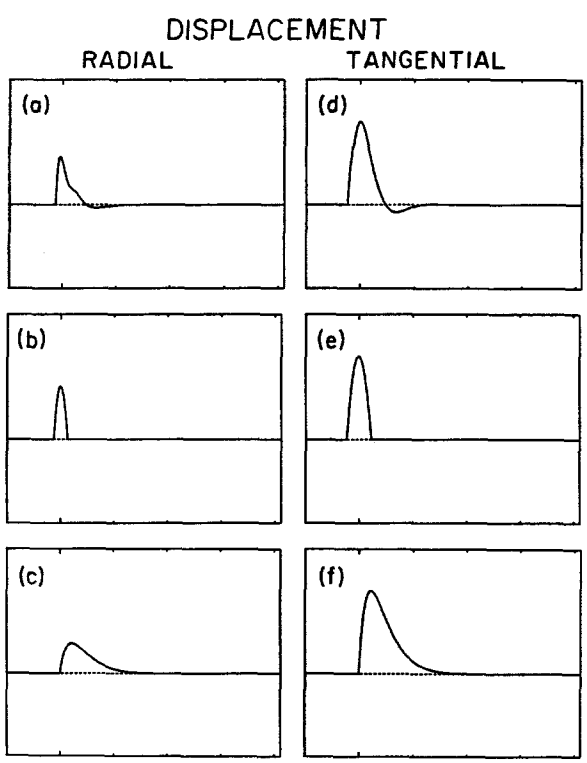

Figure 1. Far-field radial (P) and tangential (S) displacement time histories for the exact tectonic cavity release (Figs. 1a and 1d), for the Randall–Archambeau approximate cavity release (Figs. 1b and 1e), and for the ω-square double-couple model (Figs. 1c and 1f).

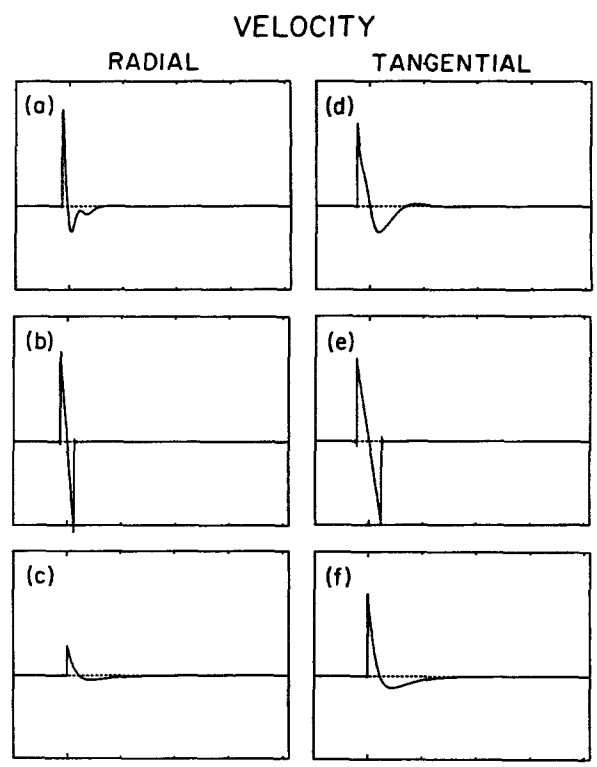

Figure 2. Far-field radial (P) and tangential (S) velocity time histories for the exact tectonic cavity release (Figs. 2a and 2d), for the Randall–Archambeau approximate cavity release (Figs. 2b and 2e), and for the ω-square double-couple model (Figs. 2c and 2f).

on the cavity release history, which corresponds in arrival time to a Rayleigh wave traveling around the cavity. The far-field displacement spectra for all four sources are shown in Figure 5 with their corresponding corner frequencies.

An Elastodynamic Potential Source in a Vertically Inhomogeneous Half-Space

An alternate method for introducing sources for which only a numerical representation exists into a vertically inhomogeneous half-space is the use of the elastodynamic representation theorem. In that technique, the numerical values for the displacement and stress of the source radiation are convolved with stress and displacement Green's functions over a surface surrounding the source. Harkrider (1981) and Bache *et al.* (1982) are early articles presenting examples of this technique for the calculation of surface waves. An important article relevant to the tectonic release problem using this technique is Day *et al.* (1987).

Because of its ease in implementation and its ability to give insight into the wave propagation effects of this source, we choose the multipole potential representation. As our source in a locally homogeneous region, we take the slightly modified elastodynamic source form of Archambeau (1968).

$$\bar{\mathbf{\Phi}}_s = -\frac{1}{k_\alpha^2}\sum_{n=0}^{\infty}\sum_{m=0}^{n}\{A_{nm}\cos m\phi + \beta_{nm}\sin m\phi\}$$

$$\cdot P_n^m(\cos\theta)\, h_n^{(2)}(k_\alpha R)$$

$$\bar{\mathbf{\Psi}}_{sj} = \frac{2}{k_\beta^2}\sum_{n=0}^{\infty}\sum_{m=0}^{n}\{C_{nm}^{(j)}\cos m\phi + D_{nm}^{(j)}\sin m\phi\}$$

$$\cdot P_n^m(\cos\theta)\, h_n^{(2)}(k_\beta R), \qquad (33)$$

where $\bar{\mathbf{\Phi}}_s$ and $\bar{\mathbf{\Psi}}_{sj}$ are the Fourier time transformed compressional and Cartesian shear potentials (j = 1, 2, and 3), respectively. In order to express these potentials in terms of the separable solutions to the Helmholtz equation in cylindrical coordinates, we use the Erdélyi integral (Harkrider, 1976; Ben-Menahem and Singh, 1981).

$$h_n^{(2)}(k_\nu R)P_n^m(\cos\theta) = \frac{(i)^{1-n}}{k_\nu}[sgn(h-z)]^{m+n}$$

$$\cdot\int_0^\infty \bar{P}_n^m\{\bar{\nu}_\nu/k_\nu\}F_\nu J_m(kr)\,kdk, \qquad (34)$$

where

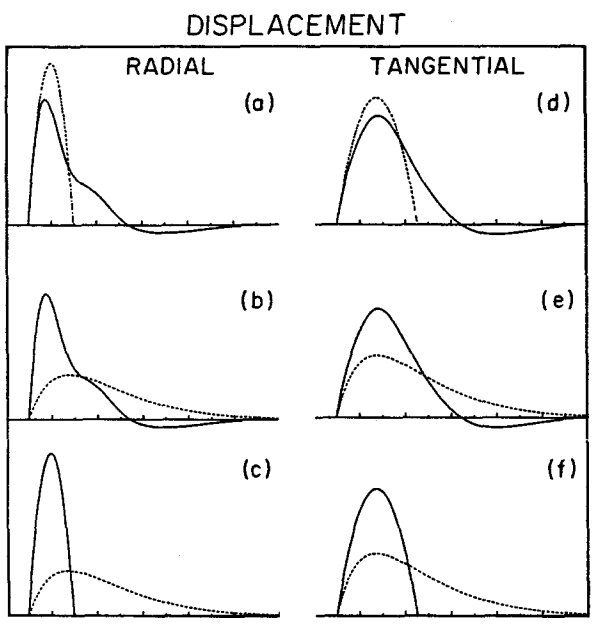

Figure 3. Far-field radial (P) and tangential (S) displacement time histories for the exact tectonic cavity release (solid line) superimposed on the Randall–Archambeau approximate cavity release (dashed line) (Figs. 3a and 3d), for the exact tectonic cavity release (solid line) superimposed on the ω-square double-couple model (dashed line) (Figs. 3b and 3e), and for the Randall–Archambeau approximate cavity release (solid line) superimposed on the ω-square double-couple model (dashed line) (Figs. 3c and 3f).

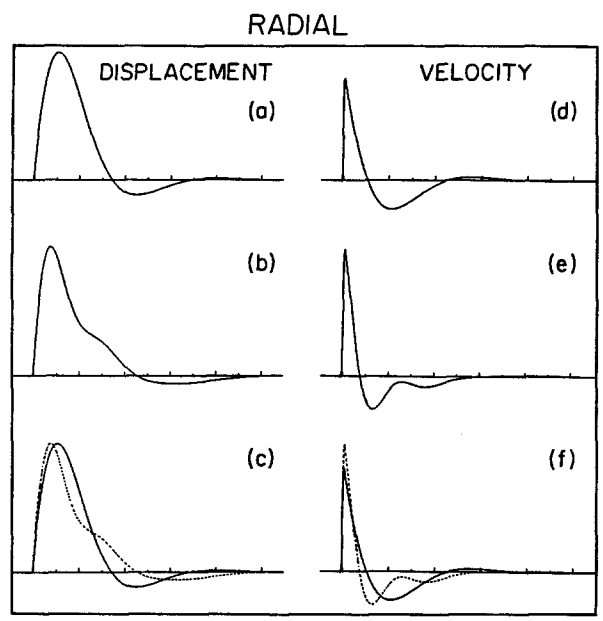

Figure 4. Far-field radial (P) displacement and velocity time histories for the step pressure on a cavity explosion (Figs. 4a and 4d), for the exact tectonic cavity release (Figs. 4b and 4e), and the two sources time histories superimposed (Figs. 4c and 4f).

$$F_\nu = k\frac{\exp(-i\tilde{\nu}_\nu|z-h|)}{i\tilde{\nu}_\nu}$$

$$\tilde{\nu}_\nu \equiv kr_\nu = \begin{cases} (k_\nu^2 - k^2)^{1/2}; & k < k_\nu \\ -i(k^2 - k_\nu^2)^{1/2}; & k > k_\nu \end{cases}$$

$$P_n^m(\xi) \equiv (1-\xi^2)^{m/2}P_n^{(m)}(\xi)$$

$$\bar{P}_n^m(\xi) \equiv (\xi^2-1)^{m/2}P_n^{(m)}(\xi)$$

$$k_\nu = \frac{\omega}{\nu}.$$

The term ν is either α or β, the compression or shear velocity, respectively, and $(r, z) = (0, h)$ is the source location.

Making use of relation (34), we can rewrite equations (33) as

$$\bar{\mathbf{\Phi}}_s = i\sum_{m=0}^{n}\int_0^\infty \{\bar{A}_m \cos m\phi + \bar{B}_m \sin m\phi\}F_\alpha J_m(kr)dk \tag{35a}$$

$$\bar{\mathbf{\Psi}}_{sj} = i\sum_{m=0}^{n}\int_0^\infty \{\bar{C}_m^{(j)} \cos m\phi + \bar{D}_m^{(j)} \sin m\phi\}F_\beta J_m(kr)dk \tag{35b}$$

where

$$\bar{A}_m = -\sum_{n=m}^{\infty}\frac{(i)^{-n}}{k_\alpha^3}[sgn(h-z)]^{m+n}A_{nm}\bar{P}_n^m\{\tilde{\nu}_\alpha/k_\alpha\}$$

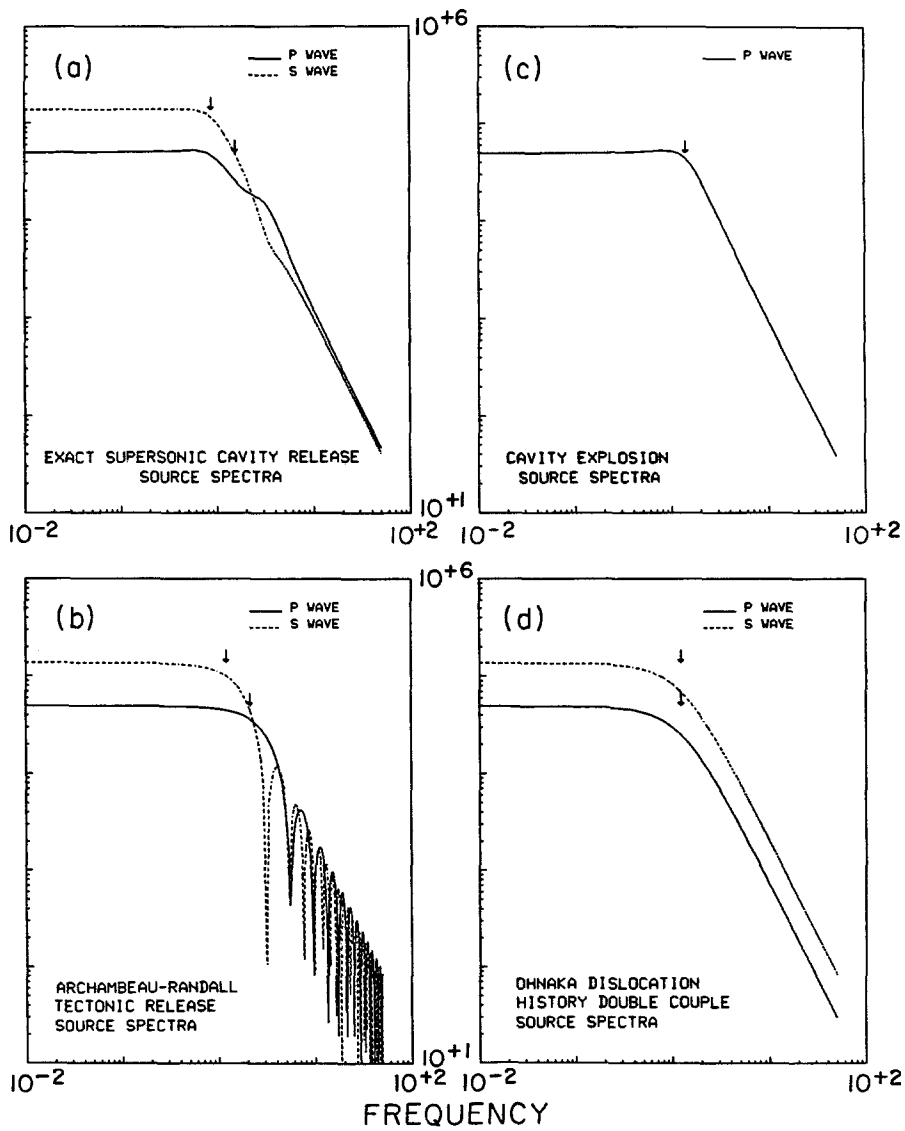

Figure 5. Far-field source displacement spectra.

$$\bar{B}_m = -\sum_{n=m}^{\infty} \frac{(i)^{-n}}{k_\alpha^3} [sgn(h-z)]^{m+n} B_{nm} \bar{P}_n^m\{\tilde{\nu}_\alpha/k_\alpha\}$$

$$\bar{C}_m^{(j)} = 2\sum_{n=m}^{\infty} \frac{(i)^{-n}}{k_\beta^3} [sgn(h-z)]^{m+n} C_{nm}^{(j)} \bar{P}_n^m\{\tilde{\nu}_\beta/k_\beta\}$$

$$\bar{D}_m^{(j)} = 2\sum_{n=m}^{\infty} \frac{(i)^{-n}}{k_\beta^3} [sgn(h-z)]^{m+n} D_{nm}^{(j)} \bar{P}_n^m\{\tilde{\nu}_\beta/k_\beta\}. \quad (36)$$

Next, we obtain expressions for the cylindrical *SV* potential, ψ, and the cylindrical *SH* potential, χ, which are convenient potentials for our cylindrical coordinate system, in terms of Cartesian *SV* and *SH* potentials given in equation (35). The relation between the wavenumber, k, integrands of the cylindrical and Cartesian potentials is derived in Appendix B and is

$$\Psi = \frac{1}{k^2}\left(\frac{\partial \Psi_2}{\partial x} - \frac{\partial \Psi_1}{\partial y}\right). \quad (37a)$$

From Harkrider (1976), the integrands of the cylindrical and Cartesian *SH* potential are related by

$$\chi = \frac{1}{k^2}(k_\beta^2 \Psi_3). \quad (37b)$$

Performing the operation, equation (37a), and comparing with the cylindrical *SV* potential

$$\bar{\Psi}_s = i\sum_{m=0}^{n} \int_0^\infty \{\bar{E}_m \cos m\phi + \bar{F}_m \sin m\phi\} F_\beta J_m(kr) dk, \quad (38)$$

we obtain the following relation between the integrand coefficients.

$$2k\bar{E}_m = (\bar{C}_{m+1}^{(2)} - \bar{C}_{m-1}^{(2)}) - (\bar{D}_{m+1}^{(1)} + \bar{D}_{m-1}^{(1)})$$

$$2k\bar{F}_m = (\bar{C}_{m+1}^{(1)} + \bar{C}_{m-1}^{(1)}) + (\bar{D}_{m+1}^{(2)} - \bar{D}_{m-1}^{(2)}), \quad (39)$$

where

$$\bar{C}_m^{(j)} \text{ and } \bar{D}_m^{(j)} \text{ are zero for } m > n,$$

and in addition,

$$C_0^{(2)} = \bar{D}_0^{(1)}, \quad \bar{C}_0^{(1)} = -\bar{D}_0^{(2)},$$

and

$$\bar{F}_0 = 0.$$

The details are given in Appendix B. For the cylindrical *SH* potential, we use equation (37b),

$$\bar{\chi}_s = i\sum_{m=0}^{n} \int_0^\infty \frac{k_\beta^2}{k^2} \{\bar{C}_m^{(3)} \cos m\phi + \bar{D}_m^{(3)} \sin m\phi\} F_\beta J_m(kr) dk. \quad (40)$$

The cylindrical source potentials given by equations (35a), (38), and (40) may now be substituted into the vertically inhomogeneous half-space formulation of Appendix A. But first we note that alternating terms in the infinite series in equations (36) are of opposite sign, depending on whether z is greater or lesser than h. We separate the series such that

$$\bar{A}_m = \bar{A}_m^e + \bar{A}_m^o, \quad (41)$$

where the e superscript denotes a new series made up of the terms with $m + n$ "even" and the o, a series formed by terms with $m + n$ "odd." A similar separation is done for the other source coefficients. The new coefficients have the following property:

$$\bar{A}_m^e(z > h) = \bar{A}_m^e(z < h)$$

and

$$\bar{A}_m^o(z > h) = -\bar{A}_m^o(z < h) \quad (42)$$

or

$$2\bar{A}_m^o = \bar{A}_m(z > h) - \bar{A}_m(z < h)$$

$$2\bar{A}_m^e = \bar{A}_m(z > h) + \bar{A}_m(z < h).$$

The Rayleigh- and Love-wave surface displacement solutions, equations (A18), (A19), and (A20) from Appendix A, for a source described in terms of source plane discontinuities in displacement and stress are

$$\{\bar{w}_o\}_R = i\frac{\pi}{k_R}\underline{A}_R \sum_{m=0}^{n} \left\{ -\delta U_1(\phi, m)\frac{1}{k_R}\bar{y}_4^R(h) - \delta U_2(\phi, m)\frac{i}{k_R}\bar{y}_2^R(h) + \delta U_3(\phi, m)\bar{y}_1^R(h) - i\delta U_4(\phi, m)\bar{y}_3^R(h) \right\} \cdot H_m^{(2)}(k_R r) \quad (43)$$

$$\{\bar{q}_o\}_R = -\frac{1}{k_R}\bar{y}_3^R(0)\frac{\partial}{\partial r}\{\bar{w}_o\}_R \tag{44}$$

with

$$\underline{A}_R = \frac{1}{2C_R U_R I_1^R},$$

where C_R is the Rayleigh wave phase velocity, U_R is the group velocity, and the energy integral is

$$I_1^R = \int_0^\infty \rho\{[\bar{y}_1^R(z)]^2 + [\bar{y}_3^R(z)]^2\}dz$$

and

$$\{\bar{v}_o\}_L = -i\frac{\pi}{k_L^2}\underline{A}_L\sum_{m=0}^{n}\left\{\delta V_2(\phi, m)\bar{y}_1^L(h) - \delta V_1(\phi, m)\frac{i}{k_L}\bar{y}_2^L(h)\right\}\frac{dH_m^{(2)}}{dr}(k_L r), \tag{45}$$

where

$$\underline{A}_L = \frac{1}{2C_L U_L I_1^L}$$

and where the Love-wave energy integral is

$$I_1^L = \int_0^\infty \rho[\bar{y}_1^L(z)]^2 dz.$$

The correspondence between the $\bar{y}_i$ notation of Saito (Saito, 1967; Takeuch and Saito, 1972; Ben-Menahem and Singh, 1981) and that of Haskell (Haskell, 1953, 1964; Harkrider, 1964, 1970; Ben-Menahem and Singh, 1981) for the eigenfunctions or the homogeneous, i.e., no source, displacement-stress vector components evaluated at the residue wavenumbers or eigenvalues is given in Appendix A. For completeness, the corresponding r_i and l_i notation of Aki and Richards, (1980, Ch. 7) is also given there. The solutions (43) and (45) are identical to equations (5.106) and (5.100) in Ben-Menahem and Singh (1981) if we associate their f_i with our δU_i, using $-f_i = \delta y_i$ and the relations between the two notations given in Appendix A.

Using equations (A4), which give $\delta U_i(\phi, m)$ and $\delta V_i(\phi, m)$ in terms of the P, SV, and SH potential coefficients of equations (35a), (38), and (40), the solutions can be written as

$$\{\bar{w}_o\}_R = -4\pi k_R\mu\underline{A}_R\left\{K_R\Phi_R^e - k_R L_R\Psi_R^e + \frac{k_R}{2\mu\nu_\alpha}M_R\Phi_R^o - \frac{k_R^2}{2\mu\nu_\beta}N_R\Psi_R^o\right\} \tag{46}$$

and

$$\{\bar{v}_o\}_L = -2\pi\mu\,\underline{A}_L\left\{\chi_L^e\bar{y}_1^L(h) - \frac{\chi_L^o}{\mu\nu_\beta}\bar{y}_2^L(h)\right\} \tag{47}$$

where

$$\nu_v = i\tilde{\nu}_v$$

$$\nu_v^2 = k^2 - k_v^2$$

$$K_R = \bar{y}_3^R(h) - \frac{1}{2\mu k_R}\bar{y}_2^R(h)$$

$$L_R = \bar{y}_1^R(h) - \frac{1}{2\mu k_R}\bar{y}_4^R(h)$$

$$M_R = \rho c_R^2(\gamma - 1)\bar{y}_1^R(h) - \frac{1}{k_R}\bar{y}_4^R(h)$$

$$N_R = \rho c_R^2(\gamma - 1)\bar{y}_3^R(h) - \frac{1}{k_R}\bar{y}_2^R(h) \tag{48}$$

$$\Phi_R^e = \sum_{m=0}^{n}(\bar{A}_m^e\cos m\phi + \bar{B}_m^e\sin m\phi)H_m^{(2)}(k_R r)$$

$$\Psi_R^e = \sum_{m=0}^{n}(\bar{E}_m^e\cos m\phi + \bar{F}_m^e\sin m\phi)H_m^{(2)}(k_R r)$$

$$\chi_L^e = \sum_{m=0}^{n}\frac{k_\beta^2}{k_L^2}(\bar{C}_m^{(3)}\cos m\phi + \bar{D}_m^{(3)e}\sin m\phi)\frac{dH_m^{(2)}}{dr}(k_L r) \tag{49}$$

and the o superscripted variables defined similarly. The elastic parameters μ and ρ, which appear in all the previous equations, except inside of integrals, are for the media at source depth h.

These last Rayleigh- and Love-wave surface displacement equations are our desired relations. Their usefulness is obvious. Since they are explicit functions of the source radiation, the contributions of the source P and S waves to the surface waves can be easily separated. From equations (42), which relate the odd, o, and even, e, superscripted factors to the source radiation above and below the source, one can use these relations to separate and evaluate the contribution to the surface waves from the upgoing and downgoing source radiation; e.g., Harkrider (1981).

Surface Waves

In order to demonstrate the utility of this formulation, once the multiple coefficients of the potentials have been determined, we first obtain the well-known surface-wave expressions for a second-order moment tensor. Then we obtain the results for our cavity release model in a pure stress field of arbitrary orientation. The result is in a form where the individual contributions of the source P and S waves are immediately recognizable. When we set the moment histories for the P and S waves equal, our expressions reduce to those for a double couple of arbitrary orientation. We also obtain the well-known result for an explosion. Finally, we reduce the tectonic release and explosion results to expressions appropriate for a shallow source, which will be used in the discussion.

The cylindrical coefficients for a second-order moment tensor are [Appendix D and equations (49)]

$$\Phi_R^e = \frac{i}{4\pi\rho\omega^2}\left\{\left[\frac{k_R^2}{2}(\bar{M}_{11}+\bar{M}_{22}) + (k_\alpha^2 - k_R^2)\bar{M}_{33}\right]\right.$$
$$\cdot H_0^{(2)}(k_R r) + \frac{k_R^2}{2}[(\bar{M}_{22}-\bar{M}_{11})\cos 2\phi$$
$$\left. - 2\bar{M}_{12}\sin 2\phi]H_2^{(2)}(k_R r)\right\}$$

$$\Phi_R^o = -\frac{i}{4\pi\rho\omega^2}2k_R\nu_\alpha[\bar{M}_{13}\cos\phi + \bar{M}_{23}\sin\phi]H_1^{(2)}(k_R r)$$

$$\Psi_R^e = \frac{i}{4\pi\rho\omega^2}\frac{(k_\beta^2 - 2k_R^2)}{k_R}[\bar{M}_{13}\cos\phi + \bar{M}_{23}\sin\phi]H_1^{(2)}(k_R r)$$

$$\Psi_R^o = \frac{i}{4\pi\rho\omega^2}\frac{\nu_\beta}{2}\{(\bar{M}_{11}+\bar{M}_{22}-2\bar{M}_{33})H_0^{(2)}(k_R r)$$
$$+ [(\bar{M}_{22}-\bar{M}_{11})\cos 2\phi - 2\bar{M}_{12}\sin 2\phi]H_2^{(2)}(k_R r)\}$$

$$\chi_L^e = \frac{i}{4\pi\rho\omega^2}\frac{k_\beta^2}{2}[2\bar{M}_{12}\cos 2\phi$$
$$+ (\bar{M}_{22}-\bar{M}_{11})\sin 2\phi]\frac{dH_2^{(2)}}{dr}(k_L r)$$

$$\chi_L^o = \frac{i}{4\pi\rho\omega^2}k_\beta^2\frac{\nu_\beta}{k_L}[\bar{M}_{23}\cos\phi - \bar{M}_{13}\sin\phi]\frac{dH_1^{(2)}}{dr}(k_L r). \tag{50}$$

Substituting these generalized cylindrical potential coefficients into equation (46), we have

$$\{\bar{w}_o\}_R = -ik_R\underline{A}_R\left\{\left[\frac{\beta^2}{\alpha^2}\frac{(\bar{M}_{11}+\bar{M}_{22}+\bar{M}_{33})}{3}K_R\right.\right.$$
$$\left. - \frac{(\bar{M}_{11}+\bar{M}_{22}-2\bar{M}_{33})}{12}B_\#\right]H_0^{(2)}(k_R r)$$
$$+ \frac{C_\#}{2}(\bar{M}_{13}\cos\phi + \bar{M}_{23}\sin\phi)H_1^{(2)}(k_R r)$$
$$+ \frac{A_\#}{4}[(\bar{M}_{11}-\bar{M}_{22})\cos 2\phi$$
$$\left. + 2\bar{M}_{12}\sin 2\phi]H_2^{(2)}(k_R r)\right\}, \tag{51}$$

where

$$A_\# = -\bar{y}_3^R(h)$$
$$B_\# = -\left\{\left(3 - 4\frac{\beta^2}{\alpha^2}\right)\bar{y}_3^R(h) + \frac{2}{\rho\alpha^2 k_R}\bar{y}_2^R(h)\right\}$$

and

$$C_\# = \frac{1}{\mu k_R}\bar{y}_4^R(h).$$

From equation (47), we obtain

$$\{\bar{v}_o\}_L = -\frac{i}{2}\underline{A}_L\left\{\frac{\bar{y}_1^L(h)}{2}[2\bar{M}_{12}\cos 2\phi\right.$$
$$+ (\bar{M}_{22}-\bar{M}_{11})\sin 2\phi]\frac{dH_2^{(2)}}{dr}(k_L r)$$
$$\left. - \frac{1}{\mu k_L}\bar{y}_2^L(h)(\bar{M}_{23}\cos\phi - \bar{M}_{13}\sin\phi)\frac{dH_1^{(2)}}{dr}(k_L r)\right\}. \tag{52}$$

The far-field forms of the above displacement fields are identical with those of Mendiguren (1977).

For a general quadrupole source of arbitrary orientation [Appendix C and equations (49)],

$$\Phi_R^e = -i\frac{\bar{M}^{(P)}(\omega)}{4\pi\rho\omega^2}\{(k_R^2 + 2\nu_\alpha^2)\Lambda_0 H_0^{(2)}(k_R r) + k_R^2\Lambda_2 H_2^{(2)}(k_R r)\}$$

$$\Phi_R^o = i\frac{\bar{M}^{(P)}(\omega)}{2\pi\rho\omega^2}k_R\nu_\alpha\Lambda_1 H_1^{(2)}(k_R r)$$

$$\Psi_R^e = -i\frac{\bar{M}^{(S)}(\omega)}{4\pi\rho\omega^2}\frac{(k_\beta^2 - 2k_R^2)}{k_R}\Lambda_1 H_1^{(2)}(k_R r)$$

$$\Psi_R^o = -i\frac{\bar{M}^{(S)}(\omega)}{4\pi\rho\omega^2}\nu_\beta\{3\,\Lambda_0 H_0^{(2)}(k_R r) + \Lambda_2 H_2^{(2)}(k_R r)\}$$

$$\chi_L^e = i\frac{\bar{M}^{(S)}(\omega)}{4\pi\rho\omega^2}\frac{k_\beta^2}{2}\frac{\partial\Lambda_2}{\partial\phi}\frac{dH_2^{(2)}}{dr}(k_L r)$$

$$\chi_L^o = -i\frac{\bar{M}^{(S)}(\omega)}{4\pi\rho\omega^2}k_\beta^2\frac{\nu_\beta}{k_L}\frac{\partial\Lambda_1}{\partial\phi}\frac{dH_1^{(2)}}{dr}(k_L r), \qquad (53)$$

where we use the P- and S-wave moment definitions

$$\bar{M}^{(P)}(\omega) = i\,4\pi\rho\omega^2\frac{K_\alpha}{k_\alpha^3}$$

$$\bar{M}^{(S)}(\omega) = i\,4\pi\rho\omega^2\frac{K_\beta}{k_\beta^3},$$

where $\tau_{12}^{(0)}$ in equations (4) are replaced by $\tau^{(0)}$, the scalar intensity of the pure shear field of arbitrary orientation (Harkrider, 1977), and

$$\Lambda_0 = \frac{1}{2}\sin\lambda\sin 2\delta$$

$$\Lambda_1 = \cos\lambda\cos\delta\cos\phi_f - \sin\lambda\cos 2\delta\sin\phi_f$$

$$\Lambda_2 = \frac{1}{2}\sin\lambda\sin 2\delta\cos 2\phi_f + \cos\lambda\sin\delta\sin 2\phi_f$$

$$\frac{\partial\Lambda_1}{\partial\phi} = -\sin\lambda\cos 2\delta\cos\phi_f - \cos\lambda\cos\delta\sin\phi_f$$

$$\frac{\partial\Lambda_2}{\partial\phi} = 2\cos\lambda\sin\delta\cos 2\phi_f - \sin\lambda\sin 2\delta\sin 2\phi_f$$

$$\phi_f = \phi - \phi_S$$

with ϕ_S the fault strike azimuth. These coefficients were defined in Harkrider (1976), Sato (1972), and used in Langston and Helmberger (1975) as A_3, A_2, A_1, A_5, and $2A_4$, respectively.

Again substituting the coefficients into equations (46) and (47), we have

$$\{\bar{w}_o\}_R = i\,k_R\underline{A}_R\frac{1}{k_\beta^2}\left\{\left[\bar{M}^{(P)}(k_R^2 + 2\nu_\alpha^2)K_R - 3\,\bar{M}^{(S)}\frac{k_R^2}{2\mu}N_R\right]\right.$$
$$\Lambda_0 H_0^{(2)}(k_R r) - \left[\bar{M}^{(P)}\frac{k_R^2}{\mu}M_R + \bar{M}^{(S)}(k_\beta^2 - 2k_R^2)L_R\right]$$
$$\Lambda_1 H_1^{(2)}(k_R r) + k_R^2\left[\bar{M}^{(P)}K_R - \bar{M}^{(S)}\frac{1}{2\mu}N_R\right]$$
$$\left.\Lambda_2 H_2^{(2)}(k_R r)\right\} \qquad (54)$$

and

$$\{\bar{v}_o\}_L = -i\frac{\bar{M}^{(S)}(\omega)}{4}A_L\left\{\bar{y}_1^L(h)\frac{\partial\Lambda_2}{\partial\phi}\frac{dH_2^{(2)}}{dr}(k_L r)\right.$$
$$\left. + \frac{2}{\mu k_L}\bar{y}_2^L(h)\frac{\partial\Lambda_1}{\partial\phi}\frac{dH_1^{(2)}}{dr}(k_L r)\right\}. \qquad (55)$$

For a double couple,

$$\bar{M}^{(P)}(\omega) = \bar{M}^{(S)}(\omega) = \bar{M}(\omega)$$

and we obtain

$$\{\bar{w}_o\}_R = -i\frac{\bar{M}(\omega)}{2}k_R\underline{A}_R\{B_\# \Lambda_0 H_0^{(2)}(k_R r)$$
$$- C_\# \Lambda_1 H_1^{(2)}(k_R r) + A_\# \Lambda_2 H_2^{(2)}(k_R r)\} \qquad (56)$$

and

$$\{\bar{v}_o\}_L = -i\frac{\bar{M}(\omega)}{4}\underline{A}_L\left\{\bar{y}_1^L(h)\frac{\partial\Lambda_2}{\partial\phi}\frac{dH_2^{(2)}}{dr}(k_L r)\right.$$
$$\left. + \frac{2}{\mu k_L}\bar{y}_2^L(h)\frac{\partial\Lambda_1}{\partial\phi}\frac{dH_1^{(2)}}{dr}(k_L r)\right\}. \qquad (57)$$

In the far-field, these expressions reduce to the double-couple expressions in Ben-Menahem and Harkrider (1964) and correct the sign error in the Love-wave coefficient $G(h)$ in Harkrider (1970), which was correctly given in Ben-Menahem and Harkrider (1964) as

$$G(h) = -\frac{1}{\mu}\left[\frac{\tau_L^*(z)}{\dot{v}_o/c}\right]_H$$

or in Saito's (1967) notation

$$G(h) = -\frac{1}{\mu k_L}\bar{y}_2^L(h).$$

For an explosion,

$$\Phi^e = \frac{i}{4\pi\rho\omega^2}k_\alpha^2\bar{M}(\omega)H_0^{(2)}(k_R r) \qquad (58)$$

and

$$\{\bar{w}_o\}_R = -ik_R\underline{A}_R\frac{\beta^2}{\alpha^2}\bar{M}(\omega)K_R H_0^{(2)}(k_R r), \qquad (59)$$

which can be obtained by either setting the diagonal components of the stress tensor equal to $\bar{M}(\omega)$ in equations (50) and (51) or by direct substitution in equation (46).

For all cases, the radial displacement is obtained from the vertical by using

$$\{\bar{q}_o\}_R = -\frac{1}{k_R}\bar{y}_3^R(0)\frac{\partial}{\partial r}\{\bar{w}_o\}_R. \tag{60}$$

For shallow sources, the source depth dependent terms reduce to

$$K_R \to \bar{y}_3^R(0)$$

$$L_R \to 1$$

$$M_R \to \rho c_R^2(\gamma - 1)$$

$$N_R \to \rho c_R^2(\gamma - 1)\,\bar{y}_3^R(0)$$

as $h \to 0$. Using

$$\rho c_R^2(\gamma - 1) = \mu(2k_R^2 - k_\beta^2)/k_R^2,$$

we have for the shallow general quadrupole source

$$\begin{aligned}\{\bar{w}_o\}_R \to i\,k_R\underline{A}_R\frac{1}{k_\beta^2}\Bigg\{\Bigg[&\bar{M}^{(P)}(3k_R^2 - 2k_\alpha^2)\\ &- \frac{3}{2}\bar{M}^{(S)}(2k_R^2 - k_\beta^2)\Bigg]\bar{y}_3^R(0)\Lambda_0 H_0^{(2)}(k_R r)\\ &- (2k_R^2 - k_\beta^2)[\bar{M}^{(P)} - \bar{M}^{(S)}]\Lambda_1 H_1^{(2)}(k_R r)\\ &+ \frac{1}{2}[2k_R^2\bar{M}^{(P)} - \bar{M}^{(S)}(2k_R^2 - k_\beta^2)]\\ &\cdot \bar{y}_3^R(0)\Lambda_2 H_2^{(2)}(k_R r)\Bigg\}\end{aligned} \tag{61}$$

and

$$\{\bar{v}_o\}_L \to -i\frac{\bar{M}^{(S)}}{4}\underline{A}_L\frac{\partial\Lambda_2}{\partial\phi}\frac{dH_2^{(2)}}{dr}(k_L r). \tag{62}$$

For the shallow explosion

$$\{\bar{w}_o\}_R \to -ik_R\underline{A}_R\frac{\beta^2}{\alpha^2}\bar{M}(\omega)\bar{y}_3^R(0)H_0^{(2)}(k_R r). \tag{63}$$

Discussion

In this section, we present synthetics of vertical Rayleigh and transverse Love waves resulting from tectonic shear stress release and an explosion. Our particular interest is in shallow sources of depths less than 1 km. Orientations of the prestress pure shear field correspond to the three canonical or "fundamental" double-couple faults: the vertical strike-slip, the vertical dip-slip, and the 45° dip thrust faults. The last fault could have been normal, but the thrust orientation corresponds to a positive rake angle less than 180° (Aki and Richards, 1980, p. 106). The thrust is also interesting because it generates Rayleigh waves, which are the negative of an explosion at all azimuths. If it occurred with an explosion, it would mask the actual size of the explosion.

Rayleigh and Love waves for two earth structures at a range of 2000 km are shown in Figure 6. The source orientations with respect to the receiver are specified by their fault equivalents, dip (δ), rake (λ), and azimuth (ϕ), and are labeled by ($\delta°$, $\lambda°$, $\phi°$). The propagation paths are for the western United States (WUS) and central United States (CUS) velocity and attenuation models determined by Wang and Herrmann (1988), (Table 1). The synthetics included a WWSSN LP instrument. Although this source represents the instantaneous or supersonic growth of a cavity in a pure shear field, we will use it to model the zone of shear failure or fracture that might be associated with underground explosions and is much larger than the actual cavity (Day *et al.*, 1987). Our maximum radius will be assumed to be equal or less than the source depth. In this example, the cavity or failure radius and source depth are both 0.8 km. This radius corresponds to *P*- and *S*-wave rise times of 0.23 and 0.39 sec for the WUS models and 0.16 and 0.28 sec for the CUS model, respectively. For comparison, we also show an explosion with the same source depth, cavity radius, and seismic moment as the tectonic release model.

The most obvious features seen in the synthetics are the differences in period content between the synthetics calculated for the two-crust upper mantle models and the poor excitation of surface waves by release in prestress field orientations corresponding to vertical dip-slip mechanisms. The longer-period Rayleigh and Love waves seen in the WUS model are partially due to the longer source rise times caused by lower source region velocities than those of the CUS model. The primary cause is the greater attenuation of the WUS model. Although the poor excitation of Rayleigh and Love waves by a near-surface vertical or horizontal dip-slip point dislocation, which are identified in the figure by (90°, 90°, 90°) and (90°, 90°, 0°), respectively, can be explained mathematically by their spectral amplitude being proportional to a stress eigenfunction that approaches zero as source depth is reduced, this is not a very intuitive

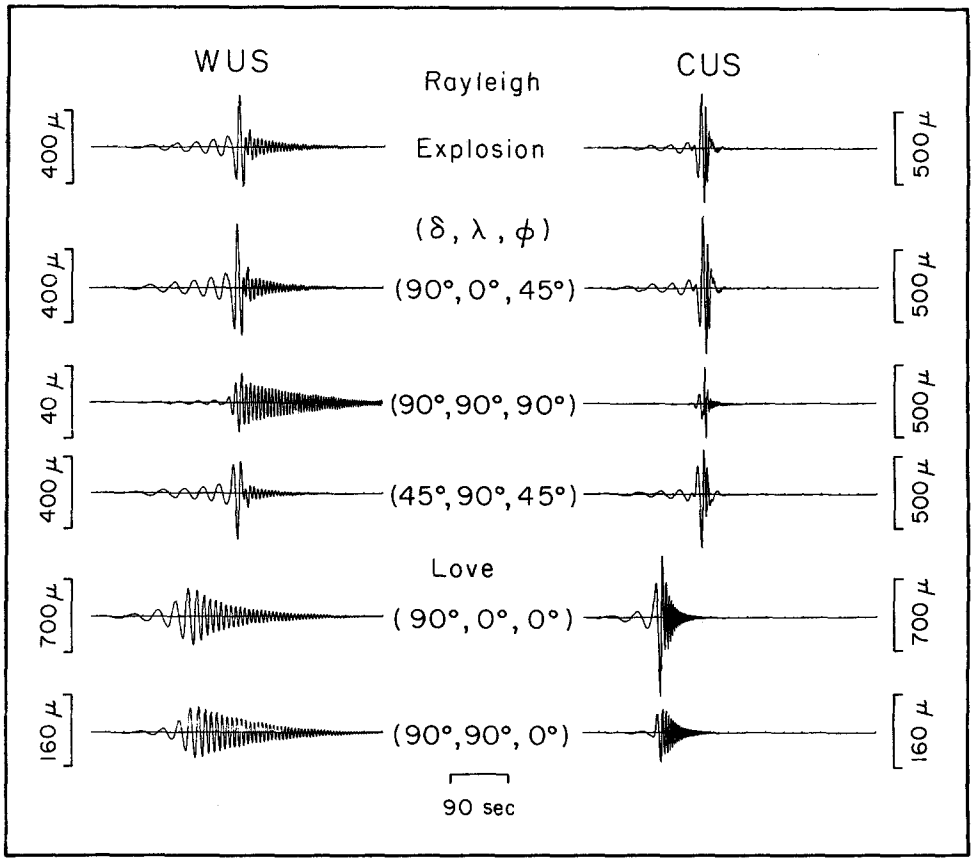

Figure 6. Vertical Rayleigh and horizontal Love waves at a range of 2000 km as observed on a WWSSN LP seismograph.

Table 1

Western United States Model (WUS)					
Thickness (km)	α (km/sec)	β (km/sec)	ρ (gm/cm^3)	Q_α	Q_β
2.0	3.55	2.06	2.20	170.0	85.0
3.0	6.15	3.27	2.79	300.0	150.0
18.0	6.15	3.57	2.79	300.0	150.0
8.0	6.70	3.93	2.97	1000.0	500.0
8.0	6.70	3.73	2.97	1000.0	500.0
0.0	7.80	4.41	3.35	2000.0	1000.0
Central United States Model (CUS)					
Thickness (km)	α (km/sec)	β (km/sec)	ρ (gm/cm^3)	Q_α	Q_β
1.0	5.00	2.89	2.5	600.0	300.0
9.0	6.10	3.52	2.7	600.0	300.0
10.0	6.40	3.70	2.9	600.0	300.0
20.0	6.70	3.87	3.0	4000.0	2000.0
0.0	8.15	4.70	3.4	4000.0	2000.0

explanation. This explanation is also frequently given for their moment tensor equivalents, $\bar{M}_{12}$ or $\bar{M}_{13}$. It would be instructive to be able to explain the observation in terms of the source vertical radiation pattern and waves generated by the free surface. For example, a frequently used ray explanation for Love and teleseismic body waves is the destructive interference between the free surface reflected waves from this shallow source and its downgoing radiation.

In order to explore the possibility of a more intuitive explanation for this near-surface effect on Rayleigh waves and to understand better the effect of differing *P*- and *SV*-wave time histories, we separated the Rayleigh wave into its contribution due to the *P* and *SV* waves separately. The resulting synthetics for the three tectonic release source orientations in the two structures are shown in Figure 7. Not only do the *P* and *SV* contributions appear to be out of phase for all the mechanisms, but the

P-wave contribution is larger for all mechanisms, except the vertical dip-slip, where it is essentially the same. The *P* contribution for the strike-slip orientation is even larger than that due to an explosion of equal moment. This is particularly evident in the CUS structure. The enhancement of the *P*-wave generated Rayleigh waves for the strike-slip over the explosion is probably due to the vertical radiation pattern or amplitude variation over the source wave front. This effect should be similar to that of the interaction of wave-front curvature with the free surface used to explain the excitation of the Rayleigh wave on a homogeneous half-space.

As mentioned above, the Rayleigh wave generated by the *P*-wave radiation from the shallow vertical dip-slip fault model is almost equal and opposite to the Rayleigh wave excited by the *SV* source radiation. Their individual amplitudes are similar to the vertical strike-slip generated Rayleigh waves. In order to demonstrate this analytically, we separate the expressions for the vertical Rayleigh-wave displacement due to this mechanism into its contribution from the *P* and *SV* source radiation. The *P* and *SV* potentials from equations (53) reduce to

$$\Phi^o = i\,\frac{\bar{M}^{(P)}(\omega)}{2\pi\rho\omega^2}\,k_R\nu_\alpha \sin\phi_f H_1^{(2)}(k_R r)$$

$$\Psi^e = -i\,\frac{\bar{M}^{(S)}(\omega)}{4\pi\rho\omega^2}\,\frac{(k_\beta^2 - 2k_R^2)}{k_R}\sin\phi_f H_1^{(2)}(k_R r).$$

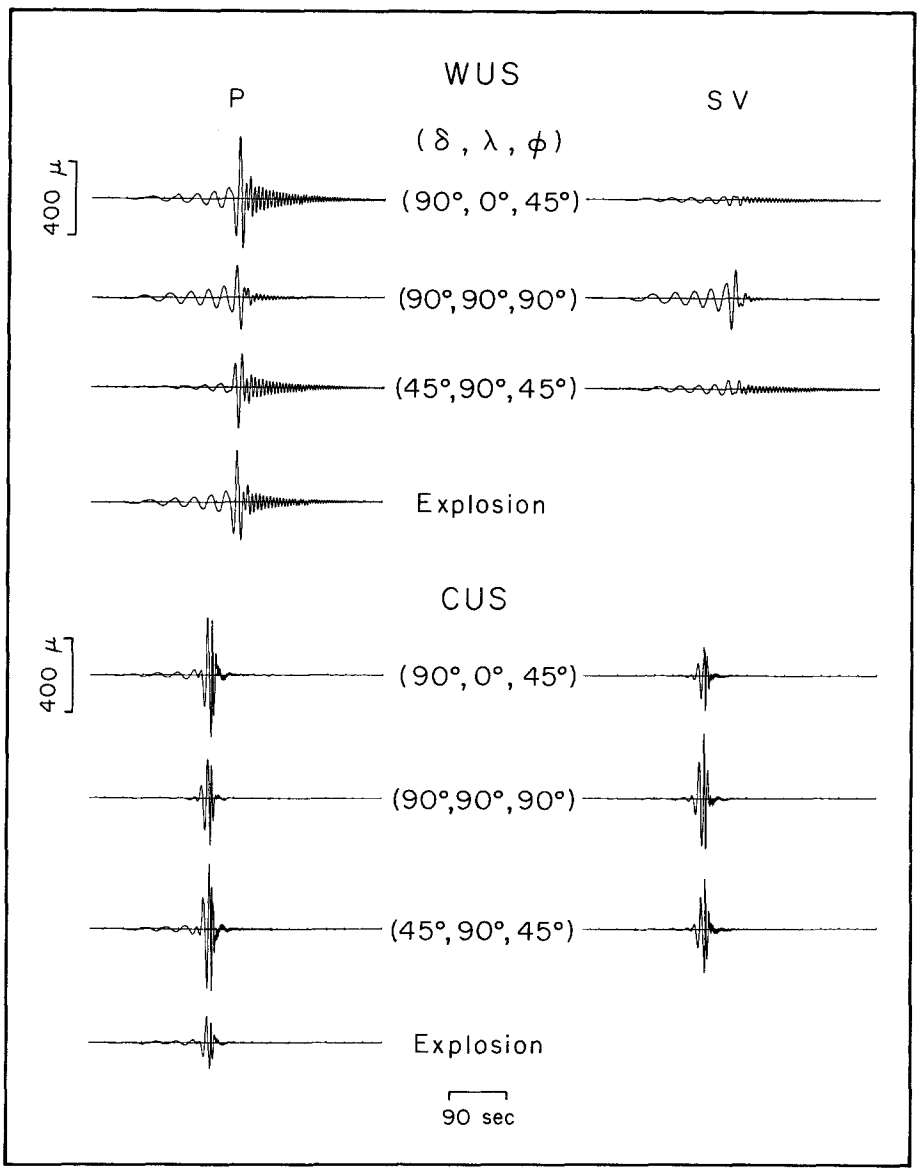

Figure 7. Vertical Rayleigh waves at a range of 2000 km as observed on a WWSSN LP seismograph. The contributions to the Rayleigh wave by the *P* and *SV* source radiation are shown separately.

Substituting the above individually into the vertical Rayleigh displacement expression (46) and recalling M_R and L_R from equations (48), we have for the vertical displacement excited by the P source potential

$$\{\bar{w}_o\}_R^{(P)} = i\frac{\bar{M}^{(P)}(\omega)}{k_\beta^2} k_R \underline{A}_R \left[(k_\beta^2 - 2k_R^2)\bar{y}_1^R(h) + \frac{k_R^2}{\mu k_R}\bar{y}_4^R(h) \right] \sin\phi_f H_1^{(2)}(k_R r) \tag{64a}$$

and the vertical displacement excited by the SV source potential

$$\{\bar{w}_o\}_R^{(SV)} = -i\frac{\bar{M}^{(S)}(\omega)}{k_\beta^2} k_R \underline{A}_R (k_\beta^2 - 2k_R^2) \cdot \left[\bar{y}_1^R(h) - \frac{1}{2\mu k_R}\bar{y}_4^R(h) \right] \sin\phi_f H_1^{(2)}(k_R r). \tag{64b}$$

If

$$\bar{M}^{(P)}(\omega) = \bar{M}^{(S)}(\omega) = \bar{M}(\omega)$$

as in a point double couple, the sum of the P and SV-wave excited Rayleigh waves reduces to the usual expression

$$\{\bar{w}_o\}_R = i\frac{\bar{M}(\omega)}{2\mu} \underline{A}_R \bar{y}_4^R(h) \sin\phi_f H_1^{(2)}(k_R r),$$

which approaches zero as the source depth $h \to 0$, since $\bar{y}_4^R(h) \to 0$, whereas

$$\{\bar{w}_o\}_R^{(P)} \to i\frac{\bar{M}^{(P)}(\omega)}{k_\beta^2} k_R \underline{A}_R (k_\beta^2 - 2k_R^2) \sin\phi_f H_1^{(2)}(k_R r)$$

and

$$\{\bar{w}_o\}_R^{(SV)} \to -i\frac{\bar{M}^{(S)}(\omega)}{k_\beta^2} k_R \underline{A}_R (k_\beta^2 - 2k_R^2) \sin\phi_f H_1^{(2)}(k_R r),$$

and their sum, which is the complete solution, approaches

$$\{\bar{w}_o\}_R \to i\frac{\bar{M}^{(P)}(\omega) - \bar{M}^{(S)}(\omega)}{k_\beta^2} k_R \underline{A}_R (k_\beta^2 - 2k_R^2) \cdot \sin\phi_f H_1^{(2)}(k_R r), \tag{65}$$

which does not vanish at zero source depth. An alternate way to derive equation (65) is to evaluate the Rayleigh-wave expression, equation (54), for a seismic quadrupole source of arbitrary orientation at an orientation corresponding to dip-slip. The tectonic release and the double couple are both members of this class of source. The resulting relation would be the sum of equations (64), which, evaluated at zero depth, is equation (65). This was not done, since we wanted expressions for the individual P- and S-wave excitation.

This surprising result for tectonic release models should be considered only as an analytic artifact, since any pure shear prestress field for this equivalent double-couple orientation, such as $\tau_{13}^{(0)}$ or $\tau_{23}^{(0)}$, where 3 is in the z direction, will be proportional to the depth below the free surface. Thus, although the displacement field for this tectonic release mechanism is not zero at the free surface for a finite moment, it is impossible for the moment to be uniform and not approach zero at shallow source depths in a realistic dip-slip prestress model. In the case of the tectonic release models, the separated expressions are actually double couples with P and SV time histories, which differ primarily by their P to SV velocity ratios in spectral amplitude and by their respective velocities in time scale (Figs. 1 through 5). We can use this tectonic release model as one way to investigate the interaction of P-and SV-generated Rayleigh waves.

The displacement expressions obtained individually for a P and a SV source, equations (64), are identical to those one would obtain by separating the displacement equation (54) into the terms that contain $\bar{M}^{(P)}$ and those that contain $\bar{M}^{(S)}$. By this means it is possible to separate the P and SV source contributions for the other orientations of the double couple as well as the tectonic release source directly from equation (54).

Similar conclusions can be reached for the case of a homogeneous half-space using the classical potential formulation where we include P- and SV-wave source potentials separately, and satisfy the boundary conditions at infinity and at the free surface for each source. For the three fundamental faults and the explosion, we have the P and SV source generated vertical surface displacements.

Vertical Strike Slip: (90°, 0°, 45°)

$$\bar{w}_o^{(P)} = \frac{\bar{M}^{(P)}}{2\pi\rho\omega^2} \int_0^\infty \frac{k^3(\gamma - 1)}{F_R} e^{-iP_s} J_2(kr)dk$$

$$\bar{w}_o^{(SV)} = \frac{\bar{M}^{(S)}}{2\pi\rho\omega^2} \int_0^\infty \frac{k^3\gamma r_\alpha r_\beta}{F_R} e^{-iQ_s} J_2(kr)dk$$

with

$$F_R = -\{(\gamma - 1)^2 + \gamma^2 r_\alpha r_\beta\}, \quad P_s = kr_\alpha h,$$

$$Q_s = kr_\beta h, \quad r_\alpha = \left(\frac{c^2}{\alpha^2} - 1\right)^{1/2},$$

$$r_\beta = \left(\frac{c^2}{\beta^2} - 1\right)^{1/2},$$

$$\gamma = 2\beta^2/c^2, \text{ and } c \equiv \omega/k.$$

Vertical Dip Slip: (90°, 90°, 90°)

$$\bar{w}_o^{(P)} = \frac{\bar{M}^{(P)}}{\pi\rho\omega^2}\int_0^\infty \frac{k^2(ikr_\alpha)(\gamma - 1)}{F_R} e^{-iP_s} J_1(kr)dk$$

$$\bar{w}_o^{(SV)} = -\frac{\bar{M}^{(S)}}{\pi\rho\omega^2}\int_0^\infty \frac{k^2(ikr_\alpha)(\gamma - 1)}{F_R} e^{-iQ_s} J_1(kr)dk.$$

45° Dip Thrust: (45°, 90°, 45°)

$$\bar{w}_o^{(P)} = \frac{\bar{M}^{(P)}}{4\pi\rho\omega^2}\int_0^\infty \frac{k(3k^2 - 2k_\alpha^2)(\gamma - 1)}{F_R} e^{-iP_s} J_0(kr)dk$$

$$\bar{w}_o^{(SV)} = \frac{\bar{M}^{(S)}}{4\pi\rho\omega^2}\int_0^\infty \frac{3k^3\gamma r_\alpha r_\beta}{F_R} e^{-iQ_s} J_0(kr)dk.$$

Explosion:

$$\bar{w}_o^{(P)} = -\frac{\bar{M}^{(P)}}{2\pi\rho\alpha^2}\int_0^\infty \frac{k(\gamma - 1)}{F_R} e^{-iP_s} J_0(kr)dk.$$

Evaluating the residue for the homogeneous half-space expressions given above, we obtain

Vertical Strike Slip: (90°, 0°, 45°)

$$\{\bar{w}_o\}_R^{(P)} = i\frac{k_R}{2}\bar{M}^{(P)}\gamma\bar{y}_3^R(0)\underline{A}_R H_2^{(2)}(k_R r)e^{-|Ps|}$$

$$\{\bar{w}_o\}_R^{(SV)} = -i\frac{k_R}{2}\bar{M}^{(S)}(\gamma - 1)\bar{y}_3^R(0)\underline{A}_R H_2^{(2)}(k_R r)e^{-|Qs|}.$$

Vertical Dip Slip: (90°, 90°, 90°)

$$\{\bar{w}_o\}_R^{(P)} = -ik_R\bar{M}^{(P)}(\gamma - 1)\underline{A}_R H_1^{(2)}(k_R r)e^{-|Ps|}$$

$$\{\bar{w}_o\}_R^{(SV)} = ik_R\bar{M}^{(S)}(\gamma - 1)\underline{A}_R H_1^{(2)}(k_R r)e^{-|Qs|}.$$

45° Dip Thrust: (45°, 90°, 45°)

$$\{\bar{w}_o\}_R^{(P)} = ik_R\bar{M}^{(P)}\frac{1}{2k_\beta^2}(3k_R^2 - 2k_\alpha^2)\bar{y}_3^R(0)\underline{A}_R H_0^{(2)}(k_R r)e^{-|Ps|}$$

$$\{\bar{w}_o\}_R^{(SV)} = -ik_R\bar{M}^{(S)}\frac{1}{2k_\beta^2}\frac{3}{2}(2k_R^2 - k_\beta^2) \cdot \bar{y}_3^R(0)\underline{A}_R H_0^{(2)}(k_R r)e^{-|Qs|}.$$

Explosion:

$$\{\bar{w}_o\}_R^{(P)} = ik_R\frac{\beta^2}{\alpha^2}\bar{M}^{(P)}\bar{y}_3^R(0)\underline{A}_R H_0^{(2)}(k_R r)e^{-|Ps|},$$

where the half-space Rayleigh response is (Harkrider, 1970; Harkrider *et al.*, 1974; Hudson and Douglas, 1975)

$$A_R = \omega\frac{1}{4\rho}\frac{r_\alpha^*}{c_R^3}\left\{(\gamma - 1) + \frac{1}{2}\frac{\gamma^3}{\alpha^2}\frac{[2c_R^2 - \alpha^2 - \beta^2]}{(\gamma - 1)^2}\right\}^{-1}$$

and the free surface ellipticity is

$$\bar{y}_3^R(0) = \frac{(\gamma - 1)}{\gamma r_\alpha^*} = \frac{r_\beta^*\gamma}{(\gamma - 1)}$$

with $r_\alpha^* = -(1 - c_R^2/\alpha^2)^{1/2}$ and $r_\beta^* = -(1 - c_R^2/\beta^2]^{1/2}$. These expressions agree with the Rayleigh-wave displacements, which one would obtain from the P and SV separated equation (61).

As the source depth, h, approaches zero, and thus P_s and Q_s approach zero, an inspection of the above expressions show that the P and SV contributions to the Rayleigh wave are of opposite sign for all the orientations and of equal amplitude for the vertical dip-slip. As stated earlier, this also can be seen for the more realistic earth models in Figure 7. Since the predicted reduction in Rayleigh-wave amplitude as a function of source depth for the vertical dip-slip source orientation is caused by a delicate balance of P- and S-wave source histories, the application of the double-couple model to shallow earthquake observations with its inherent assumption of equal P- and S-wave time histories should be done with care.

Near the surface, the stress eigenfunctions $\bar{y}_2^R$, $\bar{y}_4^R$, and $\bar{y}_2^L$ are proportional to source depth and thus vanish as the source approaches the free surface. All that remains is the $\bar{y}_1^R$, or vertical displacement eigenfunction, which controls the source depth excitation of Rayleigh waves by a vertical point force. Its excitation role is similar to the $\bar{y}_3^R$, or ellipticity eigenfunction, which governs the excitation of the horizontal point force, the shallow vertical dipole and explosions. Thus, as the vertical dip-slip oriented tectonic release source approaches the free surface, the nonvanishing part of the Rayleigh-wave amplitude can be considered as the sum of Rayleigh waves from two vertical point forces of opposite polarity; one with the P-wave time history and the other with the S-wave history. Of course, unlike azimuthally independent vertical point force Rayleigh waves, this Rayleigh wave has a sine dependence on azimuth.

The spectra for the nonvanishing Rayleigh displacement field for the shallow tectonic release sources with a vertical dip-slip orientation have a spectral minimum or hole. The spectral hole is due to the destructive interference of the P- and S-wave generated Rayleigh waves and depends on the differences in their time functions. Spectra for this difference in time functions, $|\bar{M}^{(P)} - \bar{M}^{(S)}|$, are shown in Figure 8 for a P-wave velocity of 6.2 km/cc, S-wave velocity of 3.5 km/sec, and a density of 2.7 gm/cc for our two cavity tectonic release models. The cavity radius is 0.8 km. The P- and S-wave moments are both 10^{25} dyne-cm or 10^{18} N-m. The low-frequency asymptote for the exact supersonic cavity release model is

$$\bar{M}^{(P)} - \bar{M}^{(S)} \rightarrow \frac{1}{i\omega} M_0 \frac{1}{10} \left(\frac{\omega R_0}{\alpha}\right)^2 \frac{1}{(1 - 2\sigma)}.$$

The high-frequency asymptote for the same model is

$$\bar{M}^{(P)} - \bar{M}^{(S)} \rightarrow \frac{1}{i\omega} M_0 \frac{1}{5} \left(\frac{\alpha}{\omega R_0}\right)^2 \frac{(7 - 5\sigma)}{(1 - \sigma)} \cdot \left[\exp(ik_\alpha R_0) - \frac{\beta^2}{\alpha^2} \exp(ik_\beta R_0)\right].$$

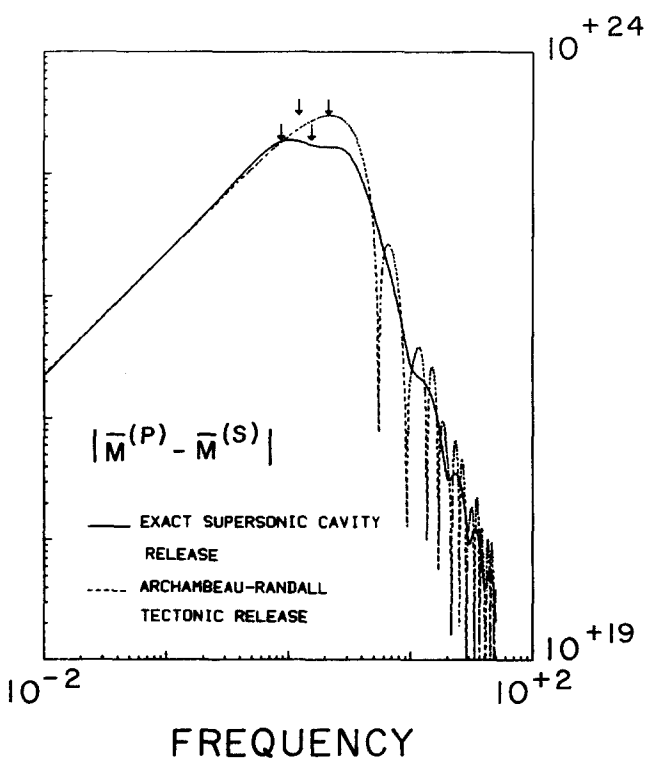

Figure 8. Spectral difference between P- and S- wave moments for the exact supersonic cavity release and the approximate Randall–Archambeau equivalent. The arrows mark the P and S corner frequencies.

The peak and the overall shape of the spectrum are controlled by the rise times or corner frequencies of the individual P- and S-wave histories. The shift to longer periods is proportional to the failure radius and inversely proportional to the body velocities. Increasing the radius also increases the peak value of this moment difference function, even if we keep the seismic moments constant. Since both moment histories have the same scalar or zero frequency moment, decreasing the size of the failure zone decreases the frequency of the Rayleigh waves most affected.

Rayleigh waves were also calculated for the vertical dip-slip orientation for source depths of 1.0, 0.8, 0.4, 0.2, and 0.0 km for a variety of cavity radii from 1.0 to 0.2 km for the WUS and CUS models. Reducing the source depth while keeping the cavity dimensions finite should be considered an analytic construction used only to demonstrate the point vertical dip-slip double-couple orientation's dependence on the difference in source P- and SV-wave time histories as the source approaches the free surface. This is particularly true for this mechanism since, as discussed earlier, the part of the prestress field, $\tau_{13}^{(0)}$ and $\tau_{23}^{(0)}$, necessary for this type of mechanism also vanishes as one approaches the free surface because of zero traction on the free surface. Even for a small source radius, the prestress will not be vertically uniform over the source dimensions. These were compared with vertical dip-slip double-couple ω-square sources with rise times equal to both the P- and the S-wave rise times of the tectonic release cases for all the source depths except the free surface. The synthetics included a WWSSN LP instrument.

For the vertical strike-slip and dip-slip orientations of tectonic release, we measured maximum peak to peak amplitudes for various release surface radii at zero source depth. As the radius was reduced, the amplitudes for the dip-slip orientation decreased monotonically. For the strike-slip model, the amplitudes increased to a maximum value and then showed a slight decrease with smaller radii for both the CUS and WUS models. This moderate maximum in the Rayleigh-wave values was felt to be due to the presence of the peak in the moment-rate spectra of the P and S waves. For rise times corresponding to the release rise times, we also measured amplitudes for the vertical strike-slip double couple at zero source depth. Since the assumed double-couple spectral history does not have a peak, decreasing the rise time or increasing the corner frequency increased the amplitude of the Rayleigh wave for both crustal models to a point at which it was the same as for a step history. As one might expect, this monotonic increase in amplitude was also observed for the dip-slip double couple at the other three source depths.

As the release radius or, equivalently, the source rise time, was reduced for the various depths, the larger Ray-

leigh-wave amplitudes approached those of the double couple. Finally, a rise time was reached such that the amplitudes of the double couple and tectonic release were identical for smaller rise times. This occurred at an *S*-wave rise time of about 0.5 sec for the CUS model at a source depth of 0.2 km. As expected, reducing the double-couple source depths by a factor of 2 reduced the Rayleigh-wave amplitude factors similarly for the vertical dip-slip model.

In addition, as the radius was decreased in the CUS model, there was a minimum amplitude at intermediate radii, which gave values less than the double couple at corresponding rise times. This was present at all depths below the surface. For the WUS model, the tectonic release values were larger for all radii and rise times. This minimum in amplitude was associated with a spectral hole present only in the tectonic release models, which was expected because of the difference in *P* and *SV* source time functions.

A compelling argument against this dip-slip effect for realistic volume or surface sources is that each of these sources can be modeled by the integration of point double couples over a surface surrounding the source. In addition, a dip-slip double couple will have a vanishing Rayleigh-wave excitation as it approaches the free surface, and thus any contribution from these double couples must come from parts of the source at depth. From this we can conclude that the magnitude of this effect is determined by the vertical extent of the source.

A more complete study of these effects would require many different elastic source and propagation structures and is beyond the scope of this article. In future studies, we recommend that investigations on the effect of tectonic release be parameterized by the duration of *P* and *SV* source histories with the restriction that the *P*- and *S*-wave seismic moments be equal and not parameterized by the time function derived from an assumed mechanism. A convenient way to approximate the effect of differing shot point velocities and source dimensions is to run a suite of double-couple time history calculations for the *P* and *SV* sources separately and then sum the different combinations. This would also allow one to check efficiently the range of source dimensions and shot point conditions for which the double couple is a valid approximation to tectonic release. From our restricted study, it was found that the double-couple model of tectonic release is valid for reasonable source rise times.

Acknowledgments

This research was supported by the Defense Advanced Research Projects Agency (DARPA) of the U.S. Department of Defense and was monitored in part by the Air Force Office of Scientific Research under Contract Number F49620-83-C-0025 and the Air Force Geophysics Laboratory under Contract Numbers F19628-85-K-0017 and F19628-87-K-0028. In addition, while at the Center of Seismic Studies, DGH and CBA received support from DARPA through the Defense Supply Service-Washington under Contract Number MDA903-84-C-0020. Contribution Number 4841, Division of Geological and Planetary Sciences, California Institute of Technology, Pasadena, California. Extensive revisions were made by DGH while at the Earth Resources Laboratory, Department of Earth, Atmospheric and Planetary Sciences, Massachussettes Institute of Technology and the Air Force Phillips Laboratory, Geophysics Directorate, Earth Science Division under support of the Air Force Office of Scientific Research through Grant Number F49620-93-1-0221.

References

Aki, K. (1967). Scaling laws of seismic spectrum, *J. Geophys. Res.* **72**, 1217–1231.

Aki, K. and P. G. Richards (1980). *Quantitative Seismology: Theory and Methods*, W. H. Freeman, San Francisco.

Aki, K. and Y. B. Tsai (1972). Mechanism of Love-wave excitation by explosive sources, *J. Geophys. Res.* **77**, 1452–1475.

Archambeau, C. B. (1968). General theory of elastodynamic source fields, *Rev. Geophys. Space Phys.* **6**, 241–288.

Archambeau, C. B. (1972). The theory of stress wave radiation from explosions in prestressed media, *Geophys. J. R. Astr. Soc.* **39**, 329–366.

Bache, T. C., S. M. Day, and H. J. Swanger (1982). Rayleigh wave synthetic seismograms from multidimensional simulations of underground explosions, *Bull. Seism. Soc. Am.* **72**, 15–28.

Bache, T. C. and D. G. Harkrider (1976). The body waves due to a general seismic source in a layered earth model: 1. formulation of the theory, *Bull. Seism. Soc. Am.* **66**, 1805–1819.

Bache, T. C., W. L. Rodi, and D. G. Harkrider (1978). Crustal structures inferred from Rayleigh wave signatures of NTS explosions, *Bull. Seism. Soc. Am.* **68**, 1399–1413.

Backus, G. and M. Mulcahy (1976). Moment tensors and other phenomenological descriptions of seismic sources—I. continuous displacements and II. discontinuous displacements, *Geophys. J. R. Astr. Soc.* **46** and **47**, 341–361 and 301–329.

Ben-Menahem, A. and D. G. Harkrider (1964). Radiation patterns of surface waves from buried dipolar point-sources in a flat stratified earth, *J. Geophys. Res.* **69**, 2605–2620.

Ben-Menahem, A. and S. J. Singh (1968a). Eigenvector expansions of Green's Dyads with applications to geophysical theory, *Geophys. J. R. Astr. Soc.* **16**, 417–452.

Ben-Menahem, A. and S. J. Singh (1968b). Multipolar elastic fields in a layered half-space, *Bull. Seism. Soc. Am.* **58**, 1519–1572.

Ben-Menahem, A. and S. J. Singh (1981). *Seismic Waves and Sources*, Springer-Verlag, New York.

Brune, J. N. (1970). Tectonic stress and the spectra of seismic shear waves from earthquakes, *J. Geophys. Res.* **75**, 4997–5009.

Burridge, R. (1975). The pulse shapes and spectra of elastic waves generated when a cavity expands in an initial shear field, *J. Geophys. Res.* **80**, 2606–2607.

Burridge, R. and Z. Alterman (1972). The elastic radiation from an expanding spherical cavity, *Geophys. J. R. Astr. Soc.* **30**, 451–477.

Day, S. M., J. T. Cherry, N. Rimer, and J. L. Stevens (1987). Nonlinear model of tectonic release from underground explosions, *Bull. Seism. Soc. Am.* **77**, 996–1016.

Doombos, D. J. (1982). Seismic moment tensors and kinematic source parameters, *Geophys. J. R. Astr. Soc.* **69**, 235–251.

Douglas, A., J. A. Hudson, and V. K. Kembhavi (1971). The analysis of surface wave spectra using a reciprocity theorem for surface waves, *Geophys. J. R. Astr. Soc.* **23**, 207–223.

Dunkin, J. W. (1965). Computation of modal solutions in layered, elastic media at high frequencies, *Bull. Seism. Soc. Am.* **55**, 335–358.

Erdélyi, A. (1937). Zur theorie der kugelwellen, *Physica* **4**, 107–120.

Gilbert, F. and G. E. Backus (1966). Propagator matrices in elastic wave and vibration problems, *Geophysics* **31**, 326–332.

Harkrider, D. G. (1964). Surface waves in multilayered elastic media, I. Rayleigh and Love waves from buried sources in a multilayered elastic half-space, *Bull. Seism. Soc. Am.* **54**, 627–679.

Harkrider, D. G. (1970). Surface waves in multilayered elastic media, Part II. Higher mode spectra and spectral ratios from point sources in plane layered earth models, *Bull. Seism. Soc. Am.* **60**, 1937–1987.

Harkrider, D. G. (1976). Potentials and displacements for two theoretical seismic sources, *Geophys. J. R. Astr. Soc.* **47**, 97–133.

Harkrider, D. G. (1977). Elastic relaxation coefficients for a spherical cavity in a prestressed medium of arbitrary orientation, *Research Note, Geophys. J. R. Astr. Soc.* **50**, 487–491.

Harkrider, D. G. (1981). Coupling near source phenomena into surface wave generation, in *Identification of Seismic Sources—Earthquake or Underground Explosion*, E. S. Huseby and S. Mykkeltveit (Editors), D. Reidel, Boston, 277–326.

Harkrider, D. G. and E. A. Flinn (1970). Effect of crustal structure on Rayleigh waves generated by atmospheric explosions, *Rev. Geophys. Space Phys.* **8**, 501–516.

Harkrider, D. G., C. A. Newton, and E. A. Flinn (1974). Theoretical effect of yield and burst height of atmospheric explosions on Rayleigh wave amplitudes, *Geophys. J. R. Astr. Soc.* **36**, 191–225.

Harvey, D. J. (1981). Seismogram synthesis using normal mode superposition: the locked mode approximation, *Geophys. J. R. Astr. Soc.* **66**, 37–69.

Haskell, N. A. (1953). The dispersion of surface waves on multilayered media, *Bull. Seism. Soc. Am.* **43**, 17–34.

Haskell, N. A. (1964). Radiation pattern of surface waves from point sources in a multilayered medium, *Bull. Seism. Soc. Am.* **54**, 377–393.

Hirasawa, T. and R. Sato (1963). Propagation of elastic waves from a spherical origin: parts 1 and 2, *Zisin* **16**, 52–77 (in Japanese).

Hudson, J. A. (1969). A quantitative evaluation of seismic signals at teleseismic distances—I. radiation from point sources, *Geophys. J. R. Astr. Soc.* **18**, 233–249.

Hudson, J. A. and A. Douglas (1975). On the amplitude of seismic waves, *Research Note, Geophys. J. R. Astr. Soc.* **42**, 1039–1044.

Kind, R. and R. I. Odom (1983). Improvements to layer matrix methods, *J. Geophys.* **53**, 127–130.

Koyama, J., S. E. Horiuchi, and T. Hirasawa (1973). Elastic waves generated from sudden vanishing of rigidity in a spherical region, *J. Phys. Earth* **21**, 213–226.

Langston, C. A. and D. V. Helmberger (1975). A procedure for modeling shallow dislocation sources, *Geophys. J. R. Astr. Soc.* **42**, 117–130.

Mendiguren, J. A. (1977). Inversion of surface wave data in source mechanism studies, *J. Geophys. Res.* **82**, 889–894.

Menke, W. (1979). Comment on "Dispersion function computations for unlimited frequency values by Anas Abo-Zena," *Geophys. J. R. Astr. Soc.* **59**, 315–323.

Minster, J. B. (1979). Near-field waveforms from an arbitrarily expanding transparent spherical cavity in a prestressed medium, *Geophys. J. R. Astr. Soc.* **56**, 81–96.

Minster, J. B. and A. Suteau (1977). Far-field waveforms from an arbitrarily expanding transparent spherical cavity in a prestressed medium, *Geophys. J. R. Astr. Soc.* **61**, 215–233.

Ohnaka, M. (1973). A physical understanding of the earthquake source mechanism, *J. Phys. Earth* **21**, 39–59.

Randall, M. J. (1966). Seismic radiation from a sudden phase transition, *J. Geophys. Res.* **71**, 5297–5302.

Randall, M. J. (1973a). Spectral peaks and earthquakes source dimension, *J. Geophys. Res.* **78**, 2609–2611.

Randall, M. J. (1973b). Low frequency spectra in seismic waves from explosions, *Geophys. J. R. Astr. Soc.* **32**, 387–388.

Saito, M. (1967). Excitation of free oscillations and surface waves by point sources in a vertically heterogeneous earth, *J. Geophys. Res.* **72**, 3689–3699.

Sato, R. (1972). Seismic waves in the near field, *J. Phys. Earth* **20**, 357–375.

Sezawa, K. and K. Kanai (1941). Transmission of arbitrary elastic waves from a spherical source, solved with operational calculus, I and II, *Bull. Earthquake Res. Inst.* **19**, 151–161 and 417–442.

Sezawa, K. and K. Kanai (1942). Transmission of arbitrary elastic waves from a spherical source, solved with operational calculus, III, *Bull. Earthquake Res. Inst.* **20**, 1–19.

Stevens, J. L. (1980). Seismic radiation from the sudden creation of a spherical cavity in an arbitrary prestressed elastic medium, *Geophys. J. R. Astr. Soc.* **61**, 303–328.

Stevens, J. L. (1982). A mode for tectonic strain release from explosions in complex prestress fields applied to anomalous seismic waves from NTS and Eastern Kazakh explosions, S-CUBED Technical Report, (SSS-R-82-5358) and (VSC-TR-82-20), Contract Number F08606-79-C-0007 submitted to DARPA, La Jolla, California.

Stump, B. W. and L. R. Johnson (1977). The determination of source properties by the linear inversion of seismograms, *Bull. Seism. Soc. Am.* **67**, 1489–1502.

Stump, B. W. and L. R. Johnson (1982). Higher degree moment tensors—the importance of source finiteness and rupture propagation on seismograms, *Geophys. J. R. Astr. Soc.* **69**, 721–743.

Takeuchi, H. and M. Saito (1972). Seismic surface waves, in *Methods in Computational Physics*, B. A. Bolt (Editor), Vol. 11, Academic Press, New York, 217–295.

Thrower, E. N. (1965). The computation of dispersion of elastic waves in layered media, *J. Sound Vibr.* **2**, 210–226.

Wang, C. Y. and R. B. Herrmann (1980). A numerical study of *P*-, *SV*-, and *SH*-wave generation in plane layered media, *Bull. Seism. Soc. Am.* **60**, 1015–1036.

Wang, C. Y. and R. B. Herrmann (1988). Synthesis of coda waves in layered medium, *Pageoph.* **128**, 7–42.

Woodhouse, J. H. (1974). Surface waves in a laterally varying layered structure, *Geophys. J. R. Astr. Soc.* **37**, 461–490.

Appendix A
A Multipolar Source in a Vertically Inhomogeneous Half-Space Formulation

If we were only interested in the surface waves, we could start with the the Rayleigh- and Love-wave results of two excellent books on quantitative seismology by Aki and Richards (1980, Ch. 7) and Ben-Menahem and Singh (1981, Ch. 5). In particular, the intermediate results of equations (5.100) for Love and (5.106) for Rayleigh waves in the latter reference are useful. These very general intermediate relations were not obtained in the former since they were only interested in deriving the surface waves from a point force and this generalization was not needed. More general seismic sources were to be obtained by multiple spatial derivatives of these surface-wave Green's functions. As pointed out in the early parts of this article, this is a tedious and unnecessary process if you have a multipole, i.e., spherical harmonic, expansion of the source.

Unfortunately, the Rayleigh-wave solutions in both

references are not derived but stated as the results of "similar" steps to the adequately detailed derivation of the *SH*- and Love-wave solutions. Also, neither reference has the *P-SV* solution from which the Rayleigh waves could be obtained as residue contributions of the wavenumber, k, integral representations. Since no exposition of the *P-SV* and Rayleigh-wave solution can be found in the easily accessible literature of the last 20 yr, we give a brief derivation. The far simplier *SH* and Love waves can be obtained by "similar" steps. The steps follow those of Harkrider (1964) and Haskell (1964) without the slavish adherence to the awkward but fairly descriptive Haskell (1953) notation used in both articles but to an even greater degree by Harkrider in later articles. The correspondence between the notation used here and that in previous articles by a variety of authors is given at various points in this Appendix.

The the wavenumber integrands of the displacement field (q, v, w), in cylindrical coordinates (r, ϕ, z), at a depth z can be written in the following form:

$$q(r, \phi, z) = \sum_{m=0}^{n} \frac{1}{k} U_1(\phi, z, m) \frac{dJ_m(kr)}{d(kr)} - \frac{i}{k} m V_1(\phi, z, m) \frac{J_m(kr)}{kr}$$

$$v(r, \phi, z) = \sum_{m=0}^{n} \frac{i}{k} V_1(\phi, z, m) \frac{dJ_m(kr)}{d(kr)} - \frac{1}{k} m U_1(\phi, z, m) \frac{J_m(kr)}{kr}$$

$$w(r, \phi, z) = \sum_{m=0}^{n} -\frac{i}{k} U_2(\phi, z, m) J_m(kr) \qquad \text{(A1)}$$

with the stresses acting on a horizontal plane at that depth

$$T_{rz}(r, \phi, z) = \sum_{m=0}^{n} i U_4(\phi, z, m) \frac{dJ_m(kr)}{d(kr)} + m V_2(\phi, z, m) \frac{J_m(kr)}{kr}$$

$$T_{\phi z}(r, \phi, z) = \sum_{m=0}^{n} - V_2(\phi, z, m) \frac{dJ_m(kr)}{d(kr)} - im U_4(\phi, z, m) \frac{J_m(kr)}{kr}$$

$$T_{zz}(r, \phi, z) = \sum_{m=0}^{n} U_3(\phi, z, m) J_m(kr) \qquad \text{(A2)}$$

where the z and ϕ dependent elements in the series are given by

$$U_i(\phi, z, m) = U_i^c(z, m) \cos m\phi + U_i^s(z, m) \sin m\phi$$

$$V_i(\phi, z, m) = V_i^c(z, m) \cos m\phi + V_i^s(z, m) \sin m\phi$$

where the c and s superscripts denote factors associated with the cosine and sine functions.

The above (z, m) dependent functions are related to the (z, m) dependent factors of the integrands of *P* and *SV* potentials by

$$U_1(z, m) = k^2 \left[\Phi(z, m) + \frac{d\Psi}{dz}(z, m) \right]$$

$$U_2(z, m) = ik \left[\frac{d\Phi}{dz}(z, m) + k^2 \Psi(z, m) \right]$$

$$U_3(z, m) = 2\mu \left[(k^2 - k_\alpha^2)\Phi(z, m) + k^2 \frac{d\Psi}{dz}(z, m) \right] - \lambda k_\alpha^2 \Phi(z, m)$$

$$U_4(z, m) = -ik\mu \left[\frac{d\Phi}{dz}(z, m) + (2k^2 - k_\beta^2) \frac{d\Psi}{dz}(z, m) \right] \qquad \text{(A3a)}$$

and to the corresponding factors in *SH* potential integrands by

$$V_1(z, m) = ik^2 \chi(z, m)$$

$$V_2(z, m) = k\mu \frac{d\chi}{dz}(z, m). \qquad \text{(A3b)}$$

These potential relations can be obtained from the displacement-potential relations in Aki and Richards (1980), equations (7.114), and their stress displacements, equations (7.115), using the fact that the potentials satisfy their respective Helmholtz equations. The relations (A3) can also be found in Harkrider (1964).

The above displacement and stress relations are almost identical to equations (7.116) of Aki and Richards (1980), except that we have summed them over m from 0 to n and they intend to eventually sum them from $-n$ to n. Their use of both positive and negative m has the advantage of being able to use $\exp(-im\phi)$ alone instead of $\sin(m\phi)$ and $\cos(m\phi)$ as we have chosen. The disadvantage is that one must eventually convert the imaginary exponents to these trigonometric functions. In this Appendix, it should be remembered that most quantities are also functions of frequency, ω, and wavenumber, k, but for brevity of notation they are left out of the expressions unless needed for clarity. Noting these differences,

the U_i and V_i are related to the integrand r_i and l_i of Aki and Richards (1980), by comparison with their equations (7.131), and to the integrand Saito notation, y_i^R and y_i^L, of Ben-Menahem and Singh (1981), by comparison with their equations (5.83), by

$$2\pi U_1(z, m) = k^2 r_1(m, z) = k^2 y_3^R(z)$$

$$2\pi U_2(z, m) = -ik^2 r_2(m, z) = -ik^2 y_1^R(z)$$

$$2\pi U_3(z, m) = -kr_4(m, z) = ky_2^R(z)$$

$$2\pi U_4(z, m) = -ir_3(m, z) = iky_4^R(z)$$

and

$$2\pi V_1(z, m) = ikl_1(m, z) = -ik^2 y_1^L(z)$$

$$2\pi V_2(z, m) = l_2(m, z) = ky_2^L(z).$$

The 4 $U_i(z, m)$ are the elements of the Thomson–Haskell *P-SV* displacement-stress vector and the 2 $V_i(z, m)$ are the elements of the *SH* displacement-stress vector of Haskell (1953). A detailed discussion of these vectors can be found in Chapters 3 and 5 of Ben-Menahem and Singh (1981) using the Haskell notation. These vectors and their propagator matrices for a homogeneous layer can be found in both reference books. One must remember from inspecting the above correspondence that the order of the stress elements are reversed in the Aki and Richards (1980) definitions, and therefore reordering of the propagator matrix elements is required for a direct comparison.

These vectors are continuous in a vertically heterogeneous medium except at source depths. It is easy to show that the discontinuity in the vectors is only due to the discontinuity in the source potentials. In other words, there is no contribution due to downgoing and upgoing waves from reflections at boundaries and velocity gradients above and below the source as they pass through the source plane. The source potentials are discontinuous because the source originates or radiates upgoing waves above the source and downgoing waves below it.

Our method of solution will be (1) to decompose this displacement-stress vector discontinuity into its m superscripted c and s components; (2) propagate the discontinuity vector for each m from the source depth, h, to the free surface and apply the free surface boundary conditions to it; (3) propagate the displacement-stress vector just below the source to some greater depth to apply the radiation condition; and (4) obtain the solution by substitution of its m components in (A1) and and their k integral.

We now define the source discontinuity vectors $\delta\mathbf{U}(\phi, m)$ and $\delta\mathbf{V}(\phi, m)$ as

$$\delta U_i(\phi, m) = U_i(\phi, h + 0, m) - U_i(\phi, h - 0, m)$$

$$\delta V_i(\phi, m) = V_i(\phi, h + 0, m) - V_i(\phi, h - 0, m)$$

where $z = h$ is the source depth. We next substitute the z- and m-dependent factors in the *P*, *SV*, and *SH* potential integrals, equations (35a), (38), and (41), respectively, into the U_i and V_i relations of equations (A3). Evaluating these just below and above the source and subtracting, we obtain

$$\delta U_1^c(m) = 2k^2\left[\frac{\bar{A}_m^o}{r_\alpha} - ik\bar{E}_m^e\right]$$

$$\delta U_1^s(m) = 2k^2\left[\frac{\bar{B}_m^o}{r_\alpha} - ik\bar{F}_m^e\right]$$

$$\delta U_2^c(m) = 2k^2\left[\bar{A}_m^e + ik\frac{\bar{E}_m^o}{r_\beta}\right]$$

$$\delta U_2^s(m) = 2k^2\left[\bar{B}_m^e + ik\frac{\bar{F}_m^o}{r_\beta}\right]$$

$$\delta U_3^c(m) = 2\rho c^2 k^2\left[(\gamma - 1)\frac{\bar{A}_m^o}{r_\alpha} - ik\gamma\bar{E}_m^e\right]$$

$$\delta U_3^s(m) = 2\rho c^2 k^2\left[(\gamma - 1)\frac{\bar{B}_m^o}{r_\alpha} - ik\gamma\bar{F}_m^e\right]$$

$$\delta U_4^c(m) = 2\rho c^2 k^2\left[-\gamma\bar{A}_m^e - ik(\gamma - 1)\frac{\bar{E}_m^o}{r_\beta}\right]$$

$$\delta U_4^s(m) = 2\rho c^2 k^2\left[-\gamma\bar{B}_m^e - ik(\gamma - 1)\frac{\bar{F}_m^o}{r_\beta}\right] \quad \text{(A4a)}$$

$$\delta V_1^c(m) = i2k_\beta^2\frac{\bar{C}_m^{(3)o}}{r_\beta}$$

$$\delta V_1^s(m) = i2k_\beta^2\frac{\bar{D}_m^{(3)o}}{r_\beta}$$

$$\delta V_2^c(m) = -i2k_\beta^2\mu\bar{C}_m^{(3)e}$$

$$\delta V_2^s(m) = -i2k_\beta^2\mu\bar{D}_m^{(3)e} \quad \text{(A4b)}$$

where we have used the even and odd notation of equation (43) and

$$\gamma = \frac{2\beta^2}{c^2}, \text{ with } \quad c \equiv \frac{\omega}{k}.$$

It should be noted that the source discontinuity vectors are not explicit functions of the source depth, h. The vectors are only functions of the source type, strength,

and the density and elastic parameters at that depth. This is the reason that we did not write them as a function of h.

From this point on, we restrict our development to the *P-SV* system and drop the ϕ and m notation, while remembering that the following is for each coefficient of sin $(m\phi)$ and cos $(m\phi)$.

In order to apply a free surface or ocean bottom boundary condition, we relate the *P-SV* source discontinuity vector with the surface or the top of the solid half-space, $z = 0$, using the 4×4 *P-SV* propagator matrix, $A_R(z_2, z_1)$, where

$$\mathbf{U}(z_2) = A_R(z_2, z_1)\mathbf{U}(z_1).$$

It should also be noted that the R and L subscripts indicate Rayleigh and Love waves, respectively, since that is how the propagator matrix was originally used in seismology even though its use now includes the complete *P-SV* and *SH* solutions. Since our derivation will only use the propagator from the surface, $z = 0$, to depths, z, we use the shorthand $A_R(z)$ and A_{RS} for $A_R(h)$.

We can now write

$$\mathbf{U}(h - 0) = A_{RS}\mathbf{U}(0),$$

relating the vector above the source to the surface elements $\mathbf{U}(0)$. Defining a new vector $\mathbf{G}$ as

$$\mathbf{G} = A_{RS}^{-1}\,\mathbf{U}(h + 0),$$

where the superscript -1 indicates the matrix inverse, and substituting the two relations into the vector discontinuity definition above, we have

$$\mathbf{U}(0) = \mathbf{G} - A_{RS}^{-1}\,\delta\mathbf{U}.$$

The z-dependent parts of the displacement solutions are the first two elements of $\mathbf{U}(0)$ and we see that $\mathbf{G}$ represents the homogeneous, i.e., no source or $\delta\mathbf{U} = 0$, part of the solution. The second term in the expression represents the inhomogeneous part, which propagates the source strength to the surface.

Our boundary condition is that the surface shear stress vanish, which requires $U_4(0) = 0$, and that the normal stress either vanish or be equal to the negative of the fluid pressure above the interface. This requires that $U_3(0) = 0$ or in the fluid case that the ratio of pressure to vertical velocity be known. The value of this ratio has been given in the literature for oceans and even atmospheres since the early years of matrix methods in seismology (e.g., Haskell, 1953; Harkrider and Flinn, 1970; *etc.*, and see also Ben-Menahem and Singh, 1981, Section 9.7). We will present this ratio here in symbolic form as P_0 and remark that it is only a function of the thickness and physical parameters associated with the fluid and, of course, (ω, k). We write this boundary condition as

$$U_3(0) = P_0U_2(0).$$

Substituting these boundary conditions in the above, we have

$$\begin{aligned} U_1(0) &= G_1 - (A_{RS}^{-1})_{1j}\delta U_j \\ U_2(0) &= G_2 - (A_{RS}^{-1})_{2j}\delta U_j \\ P_0U_2(0) &= G_3 - (A_{RS}^{-1})_{3j}\delta U_j \\ 0 &= G_4 - (A_{RS}^{-1})_{4j}\delta U_j. \end{aligned} \tag{A5}$$

In order to determine G_1 and G_2, we propagate the displacement-stress vector just below the source to a depth, D, where we apply the radiation condition. The main criterion for choosing D is that it be deep enough for all waves of interest and their structure interactions to have taken place well above D. In practice, this choice is very subjective and depends on frequency and range. Thus, at depth D,

$$\mathbf{U}(D) = A_R(D, h)\mathbf{U}(h + 0),$$

and from the definition of $\mathbf{G}$, we obtain

$$\mathbf{U}(D) = A_R(D, h)A_R(h)\mathbf{G}$$

or

$$\mathbf{U}(D) = A_R(D)\mathbf{G}.$$

This last results from the multiplication property of propagator matrices. At this point, we assume that we have a homogeneous half-space below this depth and therefore can convert our dispacement-stress vector to the *P-SV* potential vector, $\mathbf{P}(z)$. This vector contains the coefficients of the potential terms associated with P and SV waves in homogeneous regions of the half-space and is given at depth D by

$$\mathbf{P}(D) = (\Delta'', \omega'', \Delta', \omega')^T,$$

where the superscript T denotes transpose. The P and SV potentials can represent either propagating or exponential waves in the z direction, depending on the values of (ω, k). The terms Δ'' and ω'' are the coefficients of the upgoing or exponentially growing P and SV waves, respectively. The terms Δ' and ω' are the corresponding coefficients for the downgoing or exponentially decreasing waves with increasing depth.

Depending on the values of (ω, k), our radiation boundary conditions are that U_1 and $U_2 \to 0$ as $z \to \infty$

or that there be no upgoing waves below that depth. Both conditions can be accomplished by the requirement that Δ'' and ω'' be zero, or

$$\mathbf{P}(D) = (0, 0, \Delta', \omega')^T.$$

Now the potential vector and the displacement-stress vector are related by

$$\mathbf{P}(D) = T^{-1}\,\mathbf{U}(D)$$

where the T^{-1} matrix is given in Harkrider (1970). The matrix can also be obtained from the E^{-1} matrix of Haskell (1953) and Ben-Menahem and Singh (1981), equation (3.184), since it similarly relates the displacement-stress vector to the potential coefficient vector by

$$(\Delta' + \Delta'', \Delta' - \Delta'', \omega' - \omega'', \omega' + \omega'')^T = E^{-1}\,\mathbf{U}(D).$$

Substituting from above, we have

$$\mathbf{P}(D) = R\,\mathbf{G}, \tag{A6}$$

where we have defined the R matrix by

$$R = T^{-1} A_R(D).$$

When discussing multilayered media, Ben-Menahem and Singh (1981) define and frequently use the following scalars, which can be written in terms of R as

$$L = R_{11}, K = R_{12}, G = R_{13}, R = R_{14}, N = R_{21},$$

$$M = R_{22}, H = R_{23}, \text{ and } S = R_{24}.$$

We now apply our radiation boundary condition and obtain from the first two elements of equation (A6),

$$\begin{aligned} 0 &= R_{1j}G_j \\ 0 &= R_{2j}G_j \end{aligned} \tag{A7}$$

which yield

$$\begin{aligned} G_1 &= \frac{\mathbf{R}_{14}G_3 + \mathbf{R}_{15}G_4}{\mathbf{R}_{11}} \\ G_2 &= -\frac{\mathbf{R}_{12}G_3 + \mathbf{R}_{13}G_4}{\mathbf{R}_{11}}, \end{aligned} \tag{A8}$$

where $\mathbf{R}$ is the 6×6 sec compound matrix of R formed by its minors, defined here as

$$\mathbf{R}_{st} = R\begin{pmatrix} jk \\ lm \end{pmatrix} \equiv R_{jl}R_{km} - R_{jm}R_{kl}$$

where $s = 1, 2, 3, 4, 5, 6$ corresponds to pairs $jk = 12, 13, 14, 23, 24, 34$ with an identical correspondence of t to lm (Gilbert and Backus, 1966; Thrower, 1965). The $R\begin{pmatrix} jk \\ lm \end{pmatrix}$ notation is from Dunkin (1965). In the R notation, we also have the following commonly used quantities in Ben-Menahem and Singh (1981):

$$NK - LM = -\mathbf{R}_{11}$$

$$GN - HL = -\mathbf{R}_{12}$$

$$RN - SL = -\mathbf{R}_{13}$$

$$GM - HK = -\mathbf{R}_{14}.$$

Before going on, we should discuss the homogeneous contribution of $\mathbf{G}$. From above, we see that $\mathbf{G}$ can be propagated continuously all the way from the surface down to the bottom, where we force it to satisfy the radiation boundary condition. We also see from equation (A5) that it does not satisfy the surface boundary conditions unless there is no source, i.e., $\delta\mathbf{U} = 0$. Then G_3 and G_4 satisfy the traction boundary condition at the surface. Let us look at equations (A8) when $G_4 = 0$ and define the following "homogeneous" quantities, which we will denote with an H subscript:

$$\left[\frac{u_o}{w_o}\right]_H \equiv \left[\frac{G_1}{G_2}\right]_H = -\frac{\mathbf{R}_{14}}{\mathbf{R}_{12}}$$

or

$$\left[\frac{u_o}{w_o}\right]_H = -\frac{\mathbf{R}_{13}}{\mathbf{R}_{12}} \tag{A9}$$

since it can be shown that $\mathbf{R}_{13} = \mathbf{R}_{14}$ using properties of the propagator matrix inverse. Since $\left[\frac{u_o}{w_o}\right]_H$ is a pure imaginary number, it is frequently referred to as the Rayleigh wave "ellipticity." We also define

$$[P_0]_H \equiv \left[\frac{G_3}{G_2}\right]_H = -\frac{\mathbf{R}_{11}}{\mathbf{R}_{12}}. \tag{A10}$$

For the set of (ω, k) for which $\mathbf{R}_{11}$ is zero, we see that G_3 is zero, and we satisfy a free surface boundary condition since G_4 was also set to zero in order to obtain the ratios. Under these conditions, we cannot use equations (A8) to obtain the ratio G_1/G_2. But from equation (A7), we have

$$\frac{G_1}{G_2} = -\frac{R_{12}}{R_{11}}$$

and with $\mathbf{R}_{11} = 0$, or

$$\frac{R_{22}}{R_{21}} = \frac{R_{12}}{R_{11}},$$

equation (A9) reduces to the free surface relation above. Thus, equation (A9) can be used whether or not there is a fluid above the solid surface.

With these definitions, we define the normalized homogeneous *P-SV* vector and *SH* vector as

$$\left[\frac{\mathbf{U}(z)}{U_2(0)}\right]_H \equiv A_R(z)(-\mathbf{R}_{13}/\mathbf{R}_{12},\ 1,\ -\mathbf{R}_{11}/\mathbf{R}_{12},\ 0)^T \quad \text{(A11)}$$

and

$$\left[\frac{\mathbf{V}(z)}{V_1(0)}\right]_H \equiv A_L(z)(1,\ iF_L/\tilde{F}_L)^T, \quad \text{(A12)}$$

where F_L and $\tilde{F}_L$ will be defined when we return to *SH*. The *P-SV* components are normalized by the homogeneous vertical surface displacement and the *SH* components by their homogeneous surface displacement. The correspondence between this notation and the $\bar{y}_i$ notation of Saito (Saito, 1967; Takeuchi and Saito, 1972; Ben-Menahem and Singh, 1981, Ch. 2) and that of Haskell (Haskell, 1953, 1964; Harkrider, 1964, 1970; Ben-Menahem and Singh, 1981, Ch. 2, 3, and 5) for these normalized homogeneous displacement-stress vector components is

$$\left[\frac{U_1(z)}{U_2(0)}\right]_H = i\bar{y}_3^R(z) = \left[\frac{u(z)}{w_o}\right]_H$$

$$\left[\frac{U_2(z)}{U_2(0)}\right]_H = \bar{y}_1^R(z) = \left[\frac{w(z)}{w_0}\right]_H$$

$$\left[\frac{U_3(z)}{U_2(0)}\right]_H = \frac{i}{k}\bar{y}_2^R(z) = \left[\frac{\sigma(z)}{\dot{w}_o/c}\right]_H$$

$$\left[\frac{U_4(z)}{U_2(0)}\right]_H = -\frac{1}{k}\bar{y}_4^R(z) = \left[\frac{\tau_R(z)}{\dot{w}_o/c}\right]_H \quad \text{(A13)}$$

$$\left[\frac{V_1(z)}{V_1(0)}\right]_H = \bar{y}_1^L(z) = \left[\frac{v(z)}{v_o}\right]_H$$

$$\left[\frac{V_2(z)}{V_1(0)}\right]_H = \frac{i}{k}\bar{y}_2^L(z) = \left[\frac{\tau_L(z)}{\dot{v}_o/c}\right]_H \quad \text{(A14)}$$

where

$$\dot{x}/c = ikx$$

and the bar or $\bar{y}_i(z)$ denotes that the $y_i(z)$ are normalized by their respective $y_1(0)$.

The homogeneous vectors satisfy the boundary conditions at depth and are continuous across the source depth but do not satisfy the surface boundary conditions for all (ω, k). In particular, we see from equation (A11) that the *P-SV* vector only satisfies the normal stress boundary condition for the set of (ω, k) which yield a value of the ratio, $-\mathbf{R}_{11}/\mathbf{R}_{12}$ equal to P_0 or zero, i.e., $\mathbf{R}_{11} = 0$, if the boundary is a free surface. For a given ω, we denote this wavenumber as the Rayleigh-wave eigenvalue, k_R, and its associated normalized homogeneous vector as the Rayleigh-wave eigenvector. From inspection of equation (A12), the *SH* vector will only satisfy the vanishing of its associated surface shear stress when $F_L = 0$. This Love-wave eigenvalue is denoted as k_L and its normalized homogeneous vector as the Love-wave eigenvector. When written out in scalar form for these eigenvalues, the relations (A11) and (A12) correspond to equations (5.130) in Ben-Menahem and Singh (1981) with $\mathbf{R}_{11} = 0$, since their relations are for a free surface.

We are now ready to proceed. Our final step is to substitute equations (A8) into the integrands of the surface displacements, i.e., the first two relations of equations (A5), using the values of G_3 and G_4 given by the last two relations of equations (A5). Substituting $U_2(0)$ into equation (A1), we then obtain as our integral solution for the vertical displacement at the surface of our vertically inhomogeneous half-space

$$\bar{w}_o = \sum_{m=0}^{n} \int_0^\infty \left(\frac{1}{ik}\right) \frac{\mathbf{R}_{11}[A]_m + \mathbf{R}_{12}[B]_m + \mathbf{R}_{13}G_4(\phi, m)}{F_e} J_m(kr)dk \quad \text{(A15)}$$

where

$$F_e = \mathbf{R}_{11} - P_0\mathbf{R}_{12}$$

and the numerator definitions are

$$[A]_m \equiv -(A_{RS})_{43}\delta U_1(\phi, m) + (A_{RS})_{33}\delta U_2(\phi, m) - (A_{RS})_{23}\delta U_3(\phi, m) + (A_{RS})_{13}\delta U_4(\phi, m)$$

$$[B]_m \equiv (A_{RS})_{42}\delta U_1(\phi, m) - (A_{RS})_{32}\delta U_2(\phi, m) + (A_{RS})_{22}\delta U_3(\phi, m) - (A_{RS})_{12}\delta U_4(\phi, m)$$

$$G_4(\phi, m) = -(A_{RS})_{41}\delta U_1(\phi, m) + (A_{RS})_{31}\delta U_2(\phi, m) - (A_{RS})_{21}\delta U_3(\phi, m) + (A_{RS})_{11}\delta U_4(\phi, m).$$

In the numerator, we have replaced the elements of the inverse propagator matrix with elements of the propagator matrix itself using the relation

$$(A^{-1})_{jk} = (-1)^{j+k}(A)_{lp}$$

where $l = n + 1 - k$, $p = n + 1 - j$, and A is an $n \times n$ matrix (Harkrider, 1964; Menke, 1979).

Equation (A15) was presented by Wang and Herrmann (1980) in terms of Dunkin's (1965) notation. As in Haskell (1964), they left the numerator in terms of the propagator matrix from the source to the surface. Replacing elements of the propagator matrix with those of its inverse, i.e., the propagator matrix from the surface down to the source, we are able to obtain the solution in a more concise form. Collecting the terms in the numerator and using the definition of the normalized homogeneous vector elements (A11) and their relation to the Saito (1967) notation (A13), we have

$$\bar{w}_o = \sum_{m=0}^{n} \int_0^\infty \left(\frac{1}{ik}\right) \left\{ -\frac{1}{k}\,\delta U_1(\phi, m)\bar{y}_4^R(h) - \frac{i}{k}\,\delta U_2(\phi, m)\bar{y}_2^R(h) + \delta U_3(\phi, m)\bar{y}_1^R(h) - i\delta U_4(\phi, m)\bar{y}_3^R(h) \right\} \cdot \frac{\mathbf{R}_{12}}{F_e} J_m(kr)dk. \tag{A16}$$

Using similar steps, we find that the surface azimuthal displacement due to SH waves is given by

$$\bar{v}_o = \sum_{m=0}^{n} \int_0^\infty \left(\frac{1}{ik}\right) \frac{\tilde{F}_L}{F_L} \left\{ \bar{y}_1^L(h)\delta V_2(\phi, m) - \frac{i}{k}\,\bar{y}_2^L(h)\delta V_1(\phi, m) \right\} \frac{dJ_m(kr)}{d(kr)}\,dk \tag{A17}$$

where

$$\tilde{F}_L = (A_L)_{22} - (A_L)_{12}^* \mu_l r_{\beta l}^*$$

$$F_L = -(A_L)_{21}^* - (A_L)_{11}\mu_l r_{\beta l}^*$$

with the notation

$$(A_L) \equiv (A_L(D))$$

and

$$x = ix^*.$$

The only restriction on this form of the integral solutions is that at some depth the media is terminated by a homogeneous half-space commencing at depth D and the half-space variables are subscripted l.

Evaluating the residue contributions of displacement solutions, (A16) and (A17), in order to obtain the surface displacements due to Rayleigh and Love waves, respectively, yields

$$\{\bar{w}_o\}_R = i\frac{\pi}{k_R}\underline{A}_R \sum_{m=0}^{n} \left\{ -\delta U_1(\phi, m)\frac{1}{k_R}\bar{y}_4^R(h) - \delta U_2(\phi, m)\frac{i}{k_R}\bar{y}_2^R(h) + \delta U_3(\phi, m)\bar{y}_1^R(h) - i\delta U_4(\phi, m)\bar{y}_3^R(h) \right\} \cdot H_m^{(2)}(k_R r) \tag{A18}$$

$$\{\bar{q}_o\}_R = -\frac{1}{k_R}\bar{y}_3^R(0)\frac{\partial}{\partial r}\{\bar{w}_o\}_R \tag{A19}$$

where

$$\underline{A}_R = -\frac{\mathbf{R}_{12}^*}{\left[\dfrac{\partial F_e}{\partial k}\right]_\omega}$$

or equivalently in terms of energy integrals

$$\underline{A}_R = \frac{1}{2c_R U_R I_1^R}$$

where

$$I_1^R = \int_0^\infty \rho\{[\bar{y}_1^R(z)]^2 + [\bar{y}_3^R(z)]^2\}dz$$

and

$$\{\bar{v}_o\}_L = -i\frac{\pi}{k_L^2}\underline{A}_L \sum_{m=0}^{n}\left\{\delta V_2(\phi, m)\bar{y}_1^L(h) - \delta V_1(\phi, m)\frac{i}{k_L}\bar{y}_2^L(h)\right\}\frac{dH_m^{(2)}}{dr}(k_L r) \quad \text{(A20)}$$

where

$$\underline{A}_L = \frac{1}{(A_L)_{11}\left(\frac{\partial F_L}{\partial k}\right)_\omega}$$

or

$$A_L = \frac{1}{2c_L U_L I_1^L}$$

where

$$I_1^L = \int_0^\infty \rho[\bar{y}_1^L(z)]^2 dz.$$

Since the Rayleigh-wave eigenvalues are the k_R for a given ω which yield zero denominators for integral representation, equation (A16), we have from $F_e = 0$ that $P_0 = -\mathbf{R}_{11}/\mathbf{R}_{12}$. And thus, the elements of the normalized homogeneous vector of (A11) in the numerator of the Rayleigh-wave contribution satisfy all the surface boundary conditions and are indeed eigenvectors. Similarly for the Love-wave homogeneous normalized vector of equation (A12), since for the residue contribution of equation (A17), $F_L = 0$.

Appendix B
Cylindrical *SV* Potential Coefficients in Terms of Cartesian Shear Potential Coefficients

The vertical displacement integrand, w, of its k integral is related to the compressional and Cartesian *SV* potential integrands by

$$w = \frac{\partial\Phi}{\partial z} + \frac{\partial\Psi_2}{\partial x} - \frac{\partial\Psi_1}{\partial y}$$

and in terms of the compressional and *SV* potential integrands by

$$w = \frac{\partial\Phi}{\partial z} + k^2\Psi,$$

which by inspection yields the relation

$$\Psi = \frac{1}{k^2}\left(\frac{\partial\Psi_2}{\partial x} - \frac{\partial\Psi_1}{\partial y}\right).$$

In terms of cylindrical coordinate derivatives

$$k^2\Psi = \left[\cos\phi\frac{\partial\Psi_2}{\partial r} - \frac{\sin\phi}{r}\frac{\partial\Psi_2}{\partial\phi} - \sin\phi\frac{\partial\Psi_1}{\partial r} - \frac{\cos\phi}{r}\frac{\partial\Psi_1}{\partial\phi}\right]$$

where the Cartesian potential integrands are

$$\Psi_1 = i\sum_{m=0}^{n}[\bar{C}_m^{(1)}\cos m\phi + \bar{D}_m^{(1)}\sin m\phi]J_m F_\beta$$

$$\Psi_2 = i\sum_{m=0}^{n}[\bar{C}_m^{(2)}\cos m\phi + \bar{D}_m^{(2)}\sin m\phi]J_m F_\beta$$

or

$$k\Psi = i\sum_{m=0}^{n}\left\{[\bar{C}_m^{(2)}\cos\phi\cos m\phi + \bar{D}_m^{(2)}\cos\phi\sin m\phi - \bar{C}_m^{(1)}\sin\phi\cos m\phi - \bar{D}_m^{(1)}\sin\phi\sin m\phi]\frac{dJ_m}{kdr} + [\bar{C}_m^{(2)}\sin\phi\sin m\phi - \bar{D}_m^{(2)}\sin\phi\cos m\phi + \bar{C}_m^{(1)}\cos\phi\sin m\phi - \bar{D}_m^{(1)}\cos\phi\cos m\phi]m\frac{J_m}{kr}\right\}F_\beta$$

and

$$\frac{dJ_m}{d(kr)} = 1/2(J_{m-1} - J_{m+1})$$

$$m\frac{J_m}{kr} = 1/2(J_{m-1} + J_{m+1})$$

then

$$2k\Psi = i\left\{\sum_{m=0}^{n} [\bar{C}_m^{(2)} \cos (m-1)\phi + \bar{D}_m^{(2)} \sin (m-1)\phi + \bar{C}_m^{(1)} \sin (m-1)\phi - \bar{D}_m^{(1)} \cos (m-1)\phi] J_{m-1} + [-\bar{C}_m^{(2)} \cos (m+1)\phi - \bar{D}_m^{(2)} \sin (m+1)\phi + \bar{C}_m^{(1)} \sin (m+1)\phi - \bar{D}_m^{(1)} \cos (m+1)\phi]\, J_{m+1}\right\} F_\beta.$$

Collecting and identifying with

$$\Psi = i \sum_{m=0}^{n} (\bar{E}_m \cos m\phi + \bar{F}_m \sin m\phi) J_m F_\beta.$$

We have the following recurrence relation

$$2k\bar{E}_m = (\bar{C}_{m+1}^{(2)} - \bar{C}_{m-1}^{(2)}) - (\bar{D}_{m+1}^{(1)} + \bar{D}_{m-1}^{(1)})$$

$$2k\bar{F}_m = (\bar{C}_{m+1}^{(1)} + \bar{C}_{m-1}^{(1)}) + (\bar{D}_{m+1}^{(2)} - \bar{D}_{m-1}^{(2)}) \quad 1 \leqq m \leqq n$$

where $\bar{C}_m^{(j)}$ and $\bar{D}_m^{(j)}$ are zero for $m > n$ and $m < 0$ and

$$\bar{C}_o^{(2)} = \bar{D}_o^{(1)} \quad \text{and} \quad \bar{C}_o^{(1)} = -\bar{D}_o^{(2)}$$

and

$$\bar{F}_o = 0$$

As an example, when $n = 6$, we have

$$2k\bar{E}_o = \bar{C}_1^{(2)} - \bar{D}_1^{(1)}$$

$$2k\bar{E}_1 = \bar{C}_2^{(2)} - \bar{D}_2^{(1)} - 2\bar{C}_o^{(2)}$$

$$2k\bar{E}_2 = \bar{C}_3^{(2)} - \bar{D}_3^{(1)} - \bar{C}_1^{(2)} - \bar{D}_1^{(1)}$$

$$2k\bar{E}_3 = \bar{C}_4^{(2)} - \bar{D}_4^{(1)} - \bar{C}_2^{(2)} - \bar{D}_2^{(1)}$$

$$2k\bar{E}_4 = \bar{C}_5^{(2)} - \bar{D}_5^{(1)} - \bar{C}_3^{(2)} - \bar{D}_3^{(1)}$$

$$2k\bar{E}_5 = -\bar{C}_4^{(2)} - \bar{D}_4^{(1)}$$

$$2k\,\bar{E}_6 = -\bar{C}_5^{(2)} - \bar{D}_5^{(1)}$$

$$2k\bar{F}_o = 0$$

$$2k\bar{F}_1 = \bar{C}_2^{(1)} + \bar{D}_2^{(2)} + 2\bar{C}_o^{(1)}$$

$$2k\bar{F}_2 = \bar{C}_3^{(1)} + \bar{D}_3^{(2)} + \bar{C}_1^{(1)} - \bar{D}_1^{(2)}$$

$$2k\bar{F}_3 = \bar{C}_4^{(1)} + \bar{D}_4^{(2)} + \bar{C}_2^{(1)} - \bar{D}_2^{(2)}$$

$$2k\bar{F}_4 = \bar{C}_5^{(1)} + \bar{D}_5^{(2)} + \bar{C}_3^{(1)} - \bar{D}_3^{(2)}$$

$$2k\bar{F}_5 = +\bar{C}_4^{(1)} - \bar{D}_4^{(2)}$$

$$2k\bar{F}_6 = +\bar{C}_5^{(2)} - \bar{D}_5^{(1)}$$

Appendix C
Cartesian and Cylindrical Multipole Coefficients for Quadrupole Sources of Arbitrary Orientation

Comparing Harkrider (1976) equations (A8) with this article's equations (33), we obtain the following Cartesian coefficients:

$$A_{20} = -K_\alpha k_\alpha^2 \sin\lambda \sin 2\delta$$

$$A_{21} = \frac{2}{3} K_\alpha k_\alpha^2 \cos\lambda \cos\delta$$

$$A_{22} = -\frac{1}{6} K_\alpha k_\alpha^2 \sin\lambda \sin 2\delta$$

$$C_{20}^{(1)} = \frac{1}{2} K_\beta k_\beta^2 \sin\lambda \cos 2\delta$$

$$D_{21}^{(1)} = -\frac{1}{3} K_\beta k_\beta^2 \sin\lambda \sin 2\delta$$

$$D_{22}^{(1)} = \frac{1}{12} K_\beta k_\beta^2 \cos\lambda \cos\delta$$

$$C_{21}^{(2)} = \frac{1}{6} K_\beta k_\beta^2 \sin\lambda \sin 2\delta$$

$$C_{22}^{(2)} = -\frac{1}{12} K_\beta k_\beta^2 \cos\lambda \cos\delta$$

$$C_{21}^{(3)} = -\frac{1}{6} K_\beta k_\beta^2 \sin\lambda \cos 2\delta$$

$$C_{22}^{(3)} = -\frac{1}{6} K_\beta k_\beta^2 \cos\lambda \sin\delta$$

$$B_{21} = -\frac{2}{3} K_\alpha k_\alpha^2 \sin\lambda \cos 2\delta$$

$$B_{22} = -\frac{1}{3} K_\alpha k_\alpha^2 \cos\lambda \sin\delta$$

$$C_{21}^{(1)} = \frac{1}{6} K_\beta k_\beta^2 \cos\lambda \sin\delta$$

$$C_{22}^{(1)} = \frac{1}{12} K_\beta k_\beta^2 \sin\lambda \cos 2\delta$$

$$C_{20}^{(2)} = \frac{1}{2} K_\beta k_\beta^2 \cos\lambda \cos\delta$$

$$D_{21}^{(2)} = -\frac{1}{6} K_\beta k_\beta^2 \cos\lambda \sin\delta$$

$$D_{22}^{(2)} = \frac{1}{12} K_\beta k_\beta^2 \sin\lambda \cos 2\delta$$

$$D_{21}^{(3)} = -\frac{1}{6} K_\beta k_\beta^2 \cos\lambda \cos\delta$$

$$D_{22}^{(3)} = \frac{1}{12} K_\beta k_\beta^2 \sin\lambda \sin 2\delta. \qquad \text{(C1)}$$

The resultant cylindrical coefficients using Appendix B are

$$\bar{A}_0^e = \frac{1}{2k_\alpha^3} K_\alpha (k^2 + 2\nu_\alpha^2) \sin\lambda \sin 2\delta$$

$$\bar{A}_2^e = \frac{1}{2k_\alpha^3} K_\alpha k^2 \sin\lambda \sin 2\delta$$

$$\bar{A}_1^o = -\frac{2}{k_\alpha^3} K_\alpha k \nu_\alpha \cos\lambda \cos\delta$$

$$\bar{B}_2^e = \frac{1}{k_\alpha^3} K_\alpha k^2 \cos\lambda \sin\delta$$

$$\bar{B}_1^o = \frac{2}{k_\alpha^3} K_\alpha k \nu_\alpha \sin\lambda \cos 2\delta$$

$$\bar{E}_0^o = \frac{3}{2k_\beta^3} K_\beta \nu_\beta \sin\lambda \sin 2\delta$$

$$\bar{E}_2^o = \frac{1}{2k_\beta^3} K_\beta \nu_\beta \sin\lambda \sin 2\delta$$

$$\bar{E}_1^e = \frac{1}{k_\beta^3} K_\beta \frac{(k_\beta^2 - 2k^2)}{k} \cos\lambda \cos\delta$$

$$\bar{C}_1^{(3)o} = -\frac{1}{k_\beta^3} K_\beta k \nu_\beta \sin\lambda \cos 2\delta$$

$$\bar{C}_2^{(3)e} = -\frac{1}{k_\beta^3} K_\beta k^2 \cos\lambda \sin\delta$$

$$\bar{F}_2^o = \frac{1}{k_\beta^3} K_\beta \nu_\beta \cos\lambda \sin\delta$$

$$\bar{F}_1^e = -\frac{1}{k_\beta^3} K_\beta \frac{(k_\beta^2 - 2k^2)}{k} \sin\lambda \cos 2\delta$$

$$\bar{D}_1^{(3)o} = -\frac{1}{k_\beta^3} K_\beta k \nu_\beta \cos\lambda \cos\delta$$

$$\bar{D}_2^{(3)e} = \frac{1}{2k_\beta^3} K_\beta k^2 \sin\lambda \sin 2\delta \qquad \text{(C2)}$$

Appendix D
Cartesian and Cylindrical Multipole Coefficients for a Seismic Moment Tensor

The definition of the second-order seismic moment tensor is

$$u_i(x, t) = M_{pq} * \frac{\partial}{\partial \xi_q} G_{ip}$$

$$u_i(x, t) = -M_{pq} * G_{ip,q}$$

or

$$\bar{u}_i(x, \omega) = -\bar{M}_{pq}^{(\omega)} \bar{G}_{ip,q},$$

where the comma denotes differentiation with respect to the observer coordinates, x, rather than the source coordinates, ξ.

Now

$$\bar{G}_{ip,q} = \frac{1}{4\pi\rho\omega^2} \left\{ \frac{\partial^3}{\partial x_i \partial x_p \partial x_q} (A_\beta - A_\alpha) + k_\beta^2 \delta_{ip} \frac{\partial}{\partial x_q} A_\beta \right\}.$$

Now from equations (25), we have that

$$\bar{\mathbf{\Phi}} = -\frac{1}{k_\alpha^2} \frac{\partial \bar{u}_i}{\partial x_i}$$

and

$$\bar{\mathbf{\Psi}}_\mathbf{i} = \frac{1}{k_\beta^2} e_{ijk} \frac{\partial \bar{u}_k}{\partial x_j}$$

or

$$\bar{\mathbf{\Phi}} = \frac{1}{k_\alpha^2} \bar{M}_{pq} \bar{G}_{ip,qi}$$

and

$$\bar{G}_{ip,qi} = \frac{1}{4\pi\rho\omega^2}\left\{\frac{\partial^2}{\partial x_p \partial x_q}\frac{\partial^2}{\partial x_i^2}(A_\beta - A_\alpha) + k_\beta^2 \delta_{ip}\frac{\partial^2}{\partial x_q \partial x_i}A_\beta\right\}$$

and since

$$\frac{\partial^2}{\partial x_i^2}A_\nu = -k_\nu^2 A_\nu \quad \text{and} \quad \delta_{ip}\frac{\partial^2}{\partial x_q \partial x_i}A_\beta = \frac{\partial^2}{\partial x_q \partial x_p}A_\beta$$

we have

$$\bar{G}_{ip,qi} = \frac{1}{4\pi\rho\omega^2}k_\alpha^2\frac{\partial^2}{\partial x_p \partial x_q}A_\alpha.$$

Thus

$$\begin{aligned}\bar{\mathbf{\Phi}} &= \frac{1}{4\pi\rho\omega^2}\bar{M}_{pq}\frac{\partial^2}{\partial x_p \partial x_q}A_\alpha \\ &= \frac{1}{4\pi\rho\omega^2}\left\{\bar{M}_{11}\frac{\partial^2}{\partial x_1^2} + \bar{M}_{22}\frac{\partial^2}{\partial x_2^2} + \bar{M}_{33}\frac{\partial^2}{\partial x_3^2}\right. \\ &\quad + 2\bar{M}_{12}\frac{\partial^2}{\partial x_1 \partial x_2} \\ &\quad \left. + 2\bar{M}_{13}\frac{\partial^2}{\partial x_1 \partial x_3} + 2\bar{M}_{23}\frac{\partial^2}{\partial x_2 \partial x_3}\right\}A_\alpha.\end{aligned}$$

From Erdélyi (1937)

$$h_n^{(2)}(k_\nu R)P_n^m(\cos\theta)e^{im\phi} = i^{-n}(D_\nu)^m P_n^{(m)}(\partial/\partial ik_\nu z)h_0^{(2)}(k_\nu R) \tag{D1}$$

where the differential operator D_ν is defined as

$$D_\nu \equiv \frac{1}{ik_\nu}\left(\frac{\partial}{\partial x_1} + i\frac{\partial}{\partial x_2}\right).$$

Combining equation (D1) with

$$h_2^{(2)}(k_\nu R)P_2^{(0)}(\cos\theta) = \frac{i}{2k_\nu}\left(\frac{3}{k_\nu^2}\frac{\partial^2 A_\nu}{\partial x_3^2} + A_\nu\right)$$

and

$$A_\nu = -ik_\nu h_0^{(2)}(k_\nu R).$$

We have

$$\frac{\partial^2 A_\nu}{\partial x_3^2} = i\frac{k_\nu^3}{3}\{h_0^{(2)}(k_\nu R) - 2h_2^{(2)}(k_\nu R)P_2^0(\cos\theta)\}$$

$$\frac{\partial^2 A_\nu}{\partial x_1^2} = i\frac{k_\nu^3}{3}\left\{h_0^{(2)}(k_\nu R) + h_2^{(2)}(k_\nu R)\left[P_2^0(\cos\theta) - \frac{1}{2}P_2^2(\cos\theta)\cos 2\phi\right]\right\}$$

$$\frac{\partial^2 A_\nu}{\partial x_2^2} = i\frac{k_\nu^3}{3}\left\{h_0^{(2)}(k_\nu R) + h_2^{(2)}(k_\nu R)\cdot\left[P_2^0(\cos\theta) + \frac{1}{2}P_2^2(\cos\theta)\cos 2\phi\right]\right\}$$

$$\frac{\partial^2 A_\nu}{\partial x_1 \partial x_2} = -i\frac{k_\nu^3}{6}h_2^{(2)}(k_\nu R)P_2^2(\cos\theta)\sin 2\phi$$

$$\frac{\partial^2 A_\nu}{\partial x_1 \partial x_3} = -i\frac{k_\nu^3}{3}h_2^{(2)}(k_\nu R)P_2^1(\cos\theta)\cos\phi$$

$$\frac{\partial^2 A_\nu}{\partial x_2 \partial x_3} = -i\frac{k_\nu^3}{3}h_2^{(2)}(k_\nu R)P_2^1(\cos\theta)\sin\phi.$$

Comparing with the definition of the Cartesian multipole coefficients, we have

$$A_{00} = -\frac{1}{4\pi\rho\omega^2}i\frac{k_\alpha^5}{3}(\bar{M}_{11} + \bar{M}_{22} + \bar{M}_{33})$$

and

$$\begin{aligned}A_{20} &= -\frac{1}{4\pi\rho\omega^2}i\frac{k_\alpha^5}{3}(\bar{M}_{11} + \bar{M}_{22} - 2\bar{M}_{33}) \\ A_{21} &= +\frac{1}{4\pi\rho\omega^2}i\frac{k_\alpha^5}{3}2\bar{M}_{13} \\ A_{22} &= +\frac{1}{4\pi\rho\omega^2}i\frac{k_\alpha^5}{6}(\bar{M}_{11} - \bar{M}_{22}) \\ B_{21} &= +\frac{1}{4\pi\rho\omega^2}i\frac{k_\alpha^5}{3}2\bar{M}_{23} \\ B_{22} &= +\frac{1}{4\pi\rho\omega^2}i\frac{k_\alpha^5}{3}\bar{M}_{12}.\end{aligned} \tag{D2}$$

Now

$$e_{ijk}\frac{\partial \bar{u}_k}{\partial x_j} = -\bar{M}_{pq}e_{ijk}\bar{G}_{kp,qj}$$

and

$$\bar{G}_{kp,qj} = \frac{1}{4\pi\rho\omega^2}\left\{\frac{\partial^2}{\partial x_p \partial x_q}\frac{\partial^2}{\partial x_k \partial x_j}(A_\beta - A_\alpha) + k_\beta^2 \delta_{kp}\frac{\partial^2}{\partial x_q x_j} A_\beta\right\}.$$

Operating with e_{ijk}, the first term is zero since it is symmetric in (j, k), and

$$e_{ijk}\bar{G}_{kp,qj} = \frac{1}{4\pi\rho\omega^2} k_\beta^2 e_{ijp}\frac{\partial^2}{\partial x_q \partial x_j} A_\beta$$

thus

$$\bar{\mathbf{\Psi}}_i = -\frac{1}{4\pi\rho\omega^2} e_{ijp}\bar{M}_{pq}\frac{\partial^2}{\partial x_q \partial x_j} A_\beta,$$

which yields

$$\bar{\mathbf{\Psi}}_1 = -\frac{1}{4\pi\rho\omega^2}\left\{(\bar{M}_{33} - \bar{M}_{22})\frac{\partial^2}{\partial x_2 \partial x_3} + \bar{M}_{23}\left(\frac{\partial^2}{\partial x_2^2} - \frac{\partial^2}{\partial x_3^2}\right) + \bar{M}_{13}\frac{\partial^2}{\partial x_1 \partial x_2} - \bar{M}_{12}\frac{\partial^2}{\partial x_1 \partial x_3}\right\} A_\beta$$

$$\bar{\mathbf{\Psi}}_2 = -\frac{1}{4\pi\rho\omega^2}\left\{(\bar{M}_{11} - \bar{M}_{33})\frac{\partial^2}{\partial x_1 \partial x_3} + \bar{M}_{13}\left(\frac{\partial^2}{\partial x_3^2} - \frac{\partial^2}{\partial x_1^2}\right) + \bar{M}_{12}\frac{\partial^2}{\partial x_2 \partial x_3} - \bar{M}_{23}\frac{\partial^2}{\partial x_1 \partial x_2}\right\} A_\beta$$

$$\bar{\mathbf{\Psi}}_3 = -\frac{1}{4\pi\rho\omega^2}\left\{(\bar{M}_{22} - \bar{M}_{11})\frac{\partial^2}{\partial x_1 \partial x_2} + \bar{M}_{12}\left(\frac{\partial^2}{\partial x_1^2} - \frac{\partial^2}{\partial x_2^2}\right) + \bar{M}_{23}\frac{\partial^2}{\partial x_1 \partial x_3} - \bar{M}_{13}\frac{\partial^2}{\partial x_2 \partial x_3}\right\} A_\beta.$$

Comparing as before, we have

$$C_{20}^{(1)} = -\frac{1}{8\pi\rho\omega^2} i k_\beta^5 \bar{M}_{23}$$

$$C_{21}^{(1)} = -\frac{1}{8\pi\rho\omega^2} i \frac{k_\beta^5}{3}\bar{M}_{12}$$

$$D_{21}^{(1)} = -\frac{1}{8\pi\rho\omega^2} i \frac{k_\beta^5}{3}(\bar{M}_{22} - \bar{M}_{33})$$

$$C_{22}^{(1)} = -\frac{1}{8\pi\rho\omega^2} i \frac{k_\beta^5}{6}\bar{M}_{23}$$

$$D_{22}^{(1)} = +\frac{1}{8\pi\rho\omega^2} i \frac{k_\beta^5}{6}\bar{M}_{13}$$

$$C_{20}^{(2)} = +\frac{1}{8\pi\rho\omega^2} i k_\beta^5 \bar{M}_{13}$$

$$C_{21}^{(2)} = +\frac{1}{8\pi\rho\omega^2} i \frac{k_\beta^5}{3}(\bar{M}_{11} - \bar{M}_{33})$$

$$D_{21}^{(2)} = +\frac{1}{8\pi\rho\omega^2} i \frac{k_\beta^5}{3}\bar{M}_{12}$$

$$C_{22}^{(2)} = -\frac{1}{8\pi\rho\omega^2} i \frac{k_\beta^5}{6}\bar{M}_{13}$$

$$D_{22}^{(2)} = -\frac{1}{8\pi\rho\omega^2} i \frac{k_\beta^5}{6}\bar{M}_{23}$$

$$C_{20}^{(3)} = 0$$

$$C_{21}^{(3)} = +\frac{1}{8\pi\rho\omega^2} i \frac{k_\beta^5}{3}\bar{M}_{23}$$

$$D_{21}^{(3)} = -\frac{1}{8\pi\rho\omega^2} i \frac{k_\beta^5}{3}\bar{M}_{13}$$

$$C_{22}^{(3)} = +\frac{1}{8\pi\rho\omega^2} i \frac{k_\beta^5}{3}\bar{M}_{12}$$

$$D_{22}^{(3)} = -\frac{1}{8\pi\rho\omega^2} i \frac{k_\beta^5}{6}(\bar{M}_{11} - M_{22}). \tag{D3}$$

The resulting cylindrical coefficients, using Appendix B, are

$$\bar{A}_0 = +\frac{1}{4\pi\rho\omega^2}\frac{i}{2}[k^2(\bar{M}_{11} + \bar{M}_{22}) + 2\bar{M}_{33}(k_\alpha^2 - k^2)]$$

$$\bar{A}_1 = +\frac{1}{4\pi\rho\omega^2} 2\epsilon k \bar{\nu}_\alpha \bar{M}_{13}$$

$$\bar{A}_2 = +\frac{1}{4\pi\rho\omega^2}\frac{i}{2} k^2(\bar{M}_{22} - M_{11})$$

$$\bar{B}_1 = +\frac{1}{4\pi\rho\omega^2} 2\epsilon k \bar{\nu}_\alpha \bar{M}_{23}$$

$$\bar{B}_2 = -\frac{1}{4\pi\rho\omega^2} i k^2 \bar{M}_{12}$$

$$\bar{C}_0^{(3)} = 0$$

$$\bar{C}_1^{(3)} = -\frac{1}{4\pi\rho\omega^2} \epsilon k \bar{\nu}_\beta \bar{M}_{23}$$

$$\bar{C}_2^{(3)} = +\frac{i}{4\pi\rho\omega^2} k^2 \bar{M}_{12}$$

$$\bar{D}_1^{(3)} = +\frac{1}{4\pi\rho\omega^2} \epsilon k \tilde{\nu}_\beta \bar{M}_{13}$$

$$\bar{D}_2^{(3)} = -\frac{i}{8\pi\rho\omega^2} k^2 (\bar{M}_{11} - \bar{M}_{22}) \qquad \text{(D4)}$$

and

$$\bar{E}_0 = -\frac{1}{8\pi\rho\omega^2} \epsilon \tilde{\nu}_\beta (\bar{M}_{11} + \bar{M}_{22} - 2\bar{M}_{33})$$

$$\bar{E}_1 = -\frac{i}{4\pi\rho\omega^2} \frac{(2k^2 - k_\beta^2)}{k} \bar{M}_{13}$$

$$\bar{E}_2 = +\frac{1}{8\pi\rho\omega^2} \epsilon \tilde{\nu}_\beta (\bar{M}_{11} - \bar{M}_{22})$$

$$\bar{F}_1 = -\frac{i}{4\pi\rho\omega^2} \frac{(2k^2 - k_\beta^2)}{k} \bar{M}_{23}$$

$$\bar{F}_2 = +\frac{1}{4\pi\rho\omega^2} \epsilon \tilde{\nu}_\beta \bar{M}_{12}$$

where

$$\epsilon = sgn(z - h).$$

Thus, coefficients involving ϵ are odd and the other coefficients are even, in the sense of equations (42).

Seismological Laboratory
California Institute of Technology
Pasadena, California 91125
(D.G.H.)

S-Cubed, Division of
Maxwell Laboratories, Inc.
La Jolla, California 92038-1620
(J.L.S.)

Physics Department
University of Colorado
Boulder, Colorado 80309
(C.B.A.)

Manuscript received 12 February 1990.